Vortex triple rings

Hassan Aref and Martin van Buren

Citation: Physics of Fluids (1994-present) **17**, 057104 (2005); doi: 10.1063/1.1898143
View online: http://dx.doi.org/10.1063/1.1898143
View Table of Contents: http://scitation.aip.org/content/aip/journal/pof2/17/5?ver=pdfcov
Published by the AIP Publishing

Vortex triple rings

Hassan Aref[a] and Martin van Buren
Department of Engineering Science and Mechanics, College of Engineering, Virginia Tech, Blacksburg, Virginia 24061

(Received 12 October 2004; accepted 7 March 2005; published online 29 April 2005)

We determine equilibrium configurations of interacting point vortices in which identical vortices are arranged on concentric circles and/or form a set of nested regular polygons with or without a vortex at the center. A new analytical method is developed that uses moments of the vortex positions and yields particularly simple results for equilibria of this kind. A complete determination of all triple-ring equilibria is given and numerous previously unknown configurations are identified. Several equilibria previously reported in the literature, found by numerical solution, are characterized analytically. © *2005 American Institute of Physics*. [DOI: 10.1063/1.1898143]

I. INTRODUCTION

The determination of vortex patterns that move without a change of shape or size has been pursued for a long time. Kelvin called this problem area "vortex statics." More recent work has used the term "vortex crystals," since the patterns of interacting vortices in question move as if rigidly connected. A recent review[1] gives a sense of the broad variety of phenomena in which this problem has played a role, and the arsenal of mathematical techniques that has been applied to it.

In this paper the aim is to expand our analytical understanding of vortex crystals consisting of a finite number of identical point vortices. The equations of motion for such a system are well known (see the aforementioned review[1] or the monographs[2,3]):

$$\frac{d\overline{z_\alpha}}{dt} = \frac{1}{2\pi i}\sum_{\beta=1}^{N}{}' \frac{\Gamma}{z_\alpha - z_\beta}, \quad \alpha = 1,\ldots,N.$$

The notation is as follows: there are N-point vortices all of circulation or strength Γ. Each instantaneous vortex position is represented as a point in the complex plane: z_α, $\alpha = 1,\ldots,N$. The vortices move about according to Helmholtz's laws, i.e., the positions z_α are to be thought of as functions of time, and these ordinary differential equations then determine their motion. Note the complex conjugation on the left-hand sides. On the right-hand side the prime on the summation symbol reminds us to omit the singular term $\alpha=\beta$.

The problem of vortex statics arises by looking for solutions where the entire configuration moves as a rigid body. For the present case of identical vortices it may be shown[1] that only rigid body rotation is possible. In that case we have $z_\alpha(t) = z_\alpha(0)e^{i\omega t}$, where ω is the angular frequency of rotation of the vortex pattern. If this *Ansatz* is substituted in the equations of motion, they reduce to a set of algebraic equations:

$$\overline{z_\alpha} = \sum_{\beta=1}^{N}{}' \frac{1}{z_\alpha - z_\beta}, \quad \alpha = 1,\ldots,N, \tag{1}$$

for a set of stationary, complex positions $z_1,\ldots,z_N$ of the vortices. In writing Eq. (1), which is our starting point for this paper, we have chosen units such that $2\pi\omega/\Gamma = 1$. In the application to vortices in superfluid He^4 the value of this physical quantity is crucially important since a sufficiently accurate measurement of the geometry of the vortex configuration, and an accurate determination of its angular velocity of rotation, would allow the determination of $\Gamma = h/m$, where h is Planck's constant and m is the mass of a He atom. An important ingredient in making such a determination, however, is a thorough understanding of the geometry of the patterns in question and this is the problem addressed in this paper.

The notion that the vortices in a vortex crystal are arranged on a system of concentric circles has been around since the beginning. Indeed, Kelvin and his followers thought that these rigidly moving vortex patterns provided models of atoms, which were thus thought to be some kind of vortical excitations of the ether. A vortex crystal with vortices arranged on concentric circles is then reminiscent of classical pictures of electrons arranged in orbitals. Kelvin's idea inspired a considerable amount of work, in particular, a full analysis of vortices arranged in a single regular polygon by Thomson, the later discoverer of the electron.

As a recent example of relevance we mention the study[4] in which a vortex crystal was identified in the eye of hurricane Isabel. Early on the eye seemed to form a centered, regular pentagon of vortices. Then, over a 6-h period it changed, first to a regular hexagon of vortices and then back to a centered, regular pentagon.

A study of configurations with two rings of vortices was undertaken by Havelock,[5] who was particularly interested in "double alternate rings" where vortices of opposite circulation populate the two rings. For large radii these configurations approach vortex-street-like patterns and this was one motivation for Havelock's study.

A comprehensive numerical attack on the problem of stable, steady configurations of identical vortices was under-

[a]Author to whom correspondence should be addressed. Electronic mail: haref@vt.edu

taken by Campbell and Ziff[6] in a report that has since become known as the Los Alamos catalog. The report was motivated by the experimental realization of steady vortex patterns in superfluid He^4 by Yarmchuk, Gordon, and Packard.[7] Campbell and Ziff[6] suggested that they had found all linearly stable equilibria for $N \leqslant 30$, a claim that thus far has stood the test of time. Many, not to say most, of the states discovered and tabulated in the Los Alamos catalog present the visual impression of vortices arranged on concentric circles, i.e., of nested, regular polygons. It has since become clear that although many, maybe all, the stable equilibria are identified in the Los Alamos catalog, there is a great richness of unstable equilibria, few of which are included in the catalog, and many of which are quite different in appearance from a set of concentric rings. Only the simplest equilibria in the catalog and virtually none of the more complicated equilibria found since, are understood analytically. The catalog has apparently never been published in its entirety. Some of the results were published in Ref. 8.

In this paper we first develop (Sec. II) a novel method of constructing moments of Eqs. (1) that leads to a hierarchy of equations of ever increasing order that must be satisfied if the vortices form an equilibrium. We summarize this system using generating functions in Sec. III. We then explore the consequences of making the *Ansatz* that the vortices are arranged on a circle (Secs. IV and V) or on a set of nested regular polygons (Secs. VI and VII) in the relations obtained. This turns out to be very fruitful and leads to a number of conclusions, e.g., that if all the vortices are on just one circle (with a vortex at the center or not), then they must be arranged in a regular polygon, and that if the vortices are arranged on nested regular polygons, then for two and three such polygons the number of vortices in each must be the same, i.e., one can have nested regular n-gons but not, say, a regular n-gon nested within or outside a regular $2n$-gon. (One can, however, have configurations with three regular n-gons of which two have the same size but do not form a regular $2n$-gon. These configurations are determined as well.)

Introducing a geometrical representation that uses trilinear coordinates we determine the number of configurations of three nested, regular n-gons for all n, both centered and noncentered. We find that the number of these states increases to and then levels off at 16 for $n \geqslant 9$, and we provide a geometrical-analytical approach to finding all these states. We visualize the actual configurations for several values of n and show that the solutions approach "asymptotic forms" as n increases with the radii of the nested polygons given as simple functions of n.

We conclude (Sec. VIII) with some summary comments on the results obtained and their relationship to earlier work.

II. MOMENT RELATIONS

In order to attempt to solve (1) we consider the "moments"

$$M_n = \sum_{\alpha=1}^{N} z_\alpha^n \overline{z_\alpha} \tag{2}$$

and

$$N_n = \sum_{\alpha=1}^{N} z_\alpha^n. \tag{3}$$

From (1) we get by simple algebra that

$$\begin{aligned} M_n &= \sum_{\alpha=1}^{N} z_\alpha^n \overline{z_\alpha} = \sum_{\alpha=1}^{N} \sum_{\beta=1}^{N}{}' \frac{z_\alpha^n}{z_\alpha - z_\beta} = \frac{1}{2} \sum_{\alpha=1}^{N} \sum_{\beta=1}^{N}{}' \frac{z_\alpha^n - z_\beta^n}{z_\alpha - z_\beta} \\ &= \frac{1}{2} \sum_{\alpha=1}^{N} \sum_{\beta=1}^{N}{}' (z_\alpha^{n-1} + z_\alpha^{n-2} z_\beta + \cdots + z_\alpha z_\beta^{n-2} + z_\beta^{n-1}) \\ &= \frac{1}{2} \sum_{k=0}^{n-1} \sum_{\alpha=1}^{N} z_\alpha^{n-1-k} \sum_{\beta=1}^{N}{}' z_\beta^k \\ &= \frac{1}{2} \sum_{k=0}^{n-1} \sum_{\alpha=1}^{N} z_\alpha^{n-1-k} \left(\sum_{\beta=1}^{N} z_\beta^k - z_\alpha^k \right), \end{aligned}$$

or

$$M_n = \frac{1}{2} \left(\sum_{k=0}^{n-1} N_{n-1-k} N_k - n N_{n-1} \right). \tag{4}$$

Let us check this relation for the first couple of moments, $n=0$ and $n=1$, where both sides of (4) may be calculated explicitly. From the definitions and easy use of (1) we have

$$M_0 = 0, \quad M_1 = N(N-1)/2, \tag{5a}$$

$$N_0 = N, \quad N_1 = 0. \tag{5b}$$

We see that these values are consistent with (4) if we define an empty sum to be zero.

For $n=2$ we get the result

$$M_2 = \tfrac{1}{2}(2N_1 N_0 - 2N_1) = 0. \tag{6a}$$

In other words,

$$\sum_{\alpha=1}^{N} z_\alpha^2 \overline{z_\alpha} = \sum_{\alpha=1}^{N} z_\alpha |z_\alpha|^2 = 0, \tag{6b}$$

or

$$\sum_{\alpha=1}^{N} x_\alpha (x_\alpha^2 + y_\alpha^2) = \sum_{\alpha=1}^{N} y_\alpha (x_\alpha^2 + y_\alpha^2) = 0, \tag{6c}$$

and so on.

III. GENERATING FUNCTIONS

We may summarize the moment relations (4) by introducing "generating functions"

$$\mu(X) = \sum_{n=0}^{\infty} M_n X^n \tag{7}$$

and

$$\nu(X) = \sum_{n=0}^{\infty} N_n X^n. \tag{8}$$

We see that

$$\nu(X) = \sum_{\alpha=1}^{N} \sum_{n=0}^{\infty} z_\alpha^n X^n = \sum_{\alpha=1}^{N} \frac{1}{1 - Xz_\alpha}. \tag{9}$$

Similarly,

$$\mu(X) = \sum_{\alpha=1}^{N} \frac{\overline{z_\alpha}}{1 - Xz_\alpha}. \tag{10}$$

We now have the following transformations (where the prime on the internal summations means $\beta \neq \alpha$):

$$\begin{aligned}
\nu(X)^2 &= \sum_{\alpha=1}^{N} \sum_{\beta=1}^{N} \frac{1}{1 - Xz_\alpha} \frac{1}{1 - Xz_\beta} \\
&= \sum_{\alpha=1}^{N} \sum_{\beta=1}^{N}{}' \frac{1}{1 - Xz_\alpha} \frac{1}{1 - Xz_\beta} + \sum_{\alpha=1}^{N} \frac{1}{(1 - Xz_\alpha)^2} \\
&= \frac{1}{X} \sum_{\alpha=1}^{N} \sum_{\beta=1}^{N}{}' \left(\frac{1}{1 - Xz_\alpha} - \frac{1}{1 - Xz_\beta} \right) \frac{1}{z_\alpha - z_\beta} \\
&\quad + \sum_{\alpha=1}^{N} \frac{1}{(1 - Xz_\alpha)^2} \\
&= \frac{2}{X} \sum_{\alpha=1}^{N} \frac{\overline{z_\alpha}}{1 - Xz_\alpha} + \sum_{\alpha=1}^{N} \frac{1}{(1 - Xz_\alpha)^2}.
\end{aligned}$$

The first term on the right-hand side is $2\mu(X)/X$. The second may be related to

$$\begin{aligned}
\nu'(X) &= \sum_{\alpha=1}^{N} \frac{z_\alpha}{(1 - Xz_\alpha)^2} = \frac{1}{X} \sum_{\alpha=1}^{N} \frac{Xz_\alpha - 1 + 1}{(1 - Xz_\alpha)^2} \\
&= -\frac{\nu}{X} + \frac{1}{X} \sum_{\alpha=1}^{N} \frac{1}{(1 - Xz_\alpha)^2}.
\end{aligned}$$

Finally then,

$$\mu = \tfrac{1}{2} X \{ \nu^2 - X\nu' - \nu \}. \tag{11}$$

This is the generating function counterpart of the relations (4).

As a simple check on the derivation of (11) consider the case of vortices on a line, for convenience taken to be the x axis of coordinates. Then

$$\mu(X) = \sum_{\alpha=1}^{N} \frac{x_\alpha}{1 - Xx_\alpha} = \frac{1}{X} \sum_{\alpha=1}^{N} \frac{Xx_\alpha - 1 + 1}{1 - Xx_\alpha} = \frac{\nu(X) - N}{X}.$$

Consider also the polynomial $P(X) = (X - x_1) \cdots (X - x_N)$ that has roots at the locations of the vortices. It is easy to see that

$$P'(X) = P(X) \sum_{\alpha=1}^{N} \frac{1}{X - x_\alpha},$$

so we have the general relation that

$$P'\left(\frac{1}{X}\right) = XP\left(\frac{1}{X}\right) \sum_{\alpha=1}^{N} \frac{1}{1 - Xx_\alpha} = XP\left(\frac{1}{X}\right) \nu(X).$$

In the case of vortices on a line, then, Eq. (11) becomes in the first instance

$$\frac{\nu(X) - N}{X} = \frac{X}{2} [\nu(X)^2 - X\nu'(X) - \nu(X)],$$

and then

$$\begin{aligned}
u^2 \frac{P'(u)}{P(u)} - Nu = \frac{1}{2u} \Bigg\{ &\left[u \frac{P'(u)}{P(u)} \right]^2 + u \frac{d}{du} \left[u \frac{P'(u)}{P(u)} \right] \\
&- u \frac{P'(u)}{P(u)} \Bigg\},
\end{aligned}$$

where $u = 1/X$. A few elementary steps yield

$$P'' - 2uP' + 2NP = 0,$$

which is the ordinary differential equation satisfied by the Hermite polynomials, i.e., the vortices are located at the roots of the Nth Hermite polynomial. This result is well known.[1]

IV. VORTICES ON A RING

Let us apply the equation for the generating functions to the case where all vortices are situated on a single ring of radius R. By the definitions of the moments we then have $M_n = R^2 N_{n-1}$, where $M_1 = NR^2 = N(N-1)/2$, or $R^2 = (N-1)/2$. Thus,

$$\mu(X) = \tfrac{1}{2}(N - 1) X \nu(X). \tag{12}$$

Substituting this into (11) we get an ordinary differential equation (ODE) for ν,

$$X\nu' = \nu(\nu - N), \tag{13}$$

which may be integrated to give

$$\nu = \frac{N}{1 - AX^N}, \tag{14}$$

where A is a constant of integration.

The power-series expansion of (14) is

$$\nu = N + ANX^N + \cdots.$$

Thus, we conclude that if all the vortices are situated on a ring, then

$$N_1 = N_2 = \cdots = N_{N-1} = 0. \tag{15}$$

Newton's formulas for the sums of powers of the roots of a polynomial (see Sec. 68 in Ref. 9) then show that the coefficients of the polynomial

$$P(X) = (X - z_1) \cdots (X - z_N),$$

considered previously for vortices on a line, all vanish, except for the coefficient of X^N and the constant term, i.e., $P(X)$ is of the form $X^N - a$, where a is some complex number. The vortices must therefore be situated at the vertices of a regular N-gon.

We have thus established: the *only* steadily rotating con-

figuration of N identical vortices with all vortices situated on a circle is the regular N-gon.

We now have $N_N = NR^N = N[(N-1)/2]^{N/2} = AN$ in the notation of (14). Thus,

$$\nu(X) = \frac{N}{1 - \left(\frac{N-1}{2}\right)^{N/2} X^N} \tag{16}$$

for this case.

V. VORTICES ON A CENTERED RING

If $N+1$ identical vortices are in a steadily rotating configuration with N vortices on a circle of radius R and one at the center, the moments M_n, $n \geqslant 0$ (now defined using all $N+1$ vortices), have the same expressions as in the case just considered, since the vortex at the origin does not contribute. The moments $N_n, n \geqslant 1$, also have the same values as before. The value of N_0 needs to be given since 0^0 is indeterminate. We set $N_0 = N$. (M_0 is still well defined and equal to 0.)

In the transformations leading to Eq. (4) we now have

$$\begin{aligned} M_n &= \sum_{\alpha=1}^{N} z_\alpha^n \overline{z_\alpha} = \sum_{\alpha=1}^{N} z_\alpha^n \left(\frac{1}{z_\alpha} + \sum_{\beta=1}^{N}{}' \frac{1}{z_\alpha - z_\beta} \right) \\ &= N_{n-1} + \frac{1}{2} \sum_{\alpha=1}^{N} \sum_{\beta=1}^{N}{}' \frac{z_\alpha^n - z_\beta^n}{z_\alpha - z_\beta} \\ &= N_{n-1} + \frac{1}{2} \sum_{\alpha=1}^{N} \sum_{\beta=1}^{N}{}' (z_\alpha^{n-1} + z_\alpha^{n-2} z_\beta + \cdots \\ &\quad + z_\alpha z_\beta^{n-2} + z_\beta^{n-1}) \\ &= \frac{1}{2} \sum_{\alpha=1}^{N} \sum_{\beta=1}^{N} (z_\alpha^{n-1} + z_\alpha^{n-2} z_\beta + \cdots + z_\alpha z_\beta^{n-2} + z_\beta^{n-1}) \\ &\quad + \left(1 - \frac{n}{2}\right) N_{n-1}, \end{aligned}$$

or

$$M_n = \frac{1}{2} \left[\sum_{k=0}^{n-1} N_{n-1-k} N_k - (n-2) N_{n-1} \right], \tag{4'}$$

where $N_0 = N$ is implicit.

Moving on to the generating functions, we have the same expressions for $\mu(X)$ and $\nu(X)$ as in (7)–(10). A difference arises in the last line of the transformation of $\nu(X)^2$ which becomes

$$\nu(X)^2 = \frac{2}{X} \sum_{\alpha=1}^{N} \frac{\overline{z_\alpha} - \frac{1}{z_\alpha}}{1 - X z_\alpha} + \sum_{\alpha=1}^{N} \frac{1}{(1 - X z_\alpha)^2}$$

or

$$\nu(X)^2 = \frac{2}{X} \mu(X) - 2 \sum_{\alpha=1}^{N} \left(\frac{1}{1 - X z_\alpha} + \frac{1}{X z_\alpha} \right) + \sum_{\alpha=1}^{N} \frac{1}{(1 - X z_\alpha)^2}.$$

Since the vortex at the origin is stationary,

$$\sum_{\alpha=1}^{N} \frac{1}{z_\alpha} = 0, \tag{17}$$

i.e., $N_{-1} = 0$, so

$$\nu(X)^2 = \frac{2}{X} \mu(X) - 2\nu(X) + \sum_{\alpha=1}^{N} \frac{1}{(1 - X z_\alpha)^2},$$

where, as before [see the line preceding Eq. (11)],

$$\sum_{\alpha=1}^{N} \frac{1}{(1 - X z_\alpha)^2} = X \nu'(X) + \nu(X).$$

The end result in this case, then, is that

$$\mu(X) = \tfrac{1}{2} X \{ \nu^2 - X \nu' + \nu \} \tag{11'}$$

in place of (11).

We still have $M_n = R^2 N_{n-1}$, which according to (17) also works for $n = 0$. Now $M_1 = NR^2 = N(N+1)/2$, so in this case $R^2 = (N+1)/2$. Thus,

$$\mu(X) = (N+1) X \nu(X)/2. \tag{12'}$$

Substituting this into (11′) we get, once again, the ODE (13) for ν!

We thus have that the *only* steadily rotating configuration of $N+1$ identical vortices with N vortices situated on a circle and with one at the center is the centered regular N-gon.

In this case $N_N = NR^N = N[(N+1)/2]^{N/2}$. Thus,

$$\nu(X) = \frac{N}{1 - \left(\frac{N+1}{2}\right)^{N/2} X^N}. \tag{16'}$$

VI. NESTED REGULAR POLYGONS OF VORTICES

As a second example of this approach, let us consider nested, regular polygons of identical vortices. Thus, let N identical vortices be placed on p polygons with the number of vortices on polygons $s = 1, \ldots, p$ being n_s, where then $n_1 + n_2 + \cdots + n_p = N$. The positions of the vortices in the sth polygon are $R_s \exp(2\pi i \alpha_s / n_s) \exp(i\phi_s)$, $s = 1, \ldots, p$; $\alpha_s = 1, \ldots, n_s$. Here R_s is the radius of the circle through the vortices on the sth polygon, and ϕ_s is a phase that gives the amount the sth polygon is turned relative to the real axis. (We may, of course, assume that one of these phases is zero but choose to keep the formulas symmetric in all indices for now.)

With this *Ansatz* the function ν may be written down as follows:

$$\nu(X) = \sum_{s=1}^{p} \sum_{\alpha_s=1}^{n_s} \frac{1}{1 - X R_s e^{i\phi_s} e^{2\pi i \alpha_s / n_s}} = \sum_{s=1}^{p} \frac{n_s}{1 - (X R_s e^{i\phi_s})^{n_s}}.$$

Let us set

$$\nu_n(X; \zeta) = \frac{n}{1 - (X\zeta)^n}. \tag{18a}$$

Then,

$$\nu(X) = \sum_{s=1}^{p} \nu_{n_s}(X; R_s e^{i\phi_s}). \tag{18b}$$

Similarly,

$$\mu(X) = \sum_{s=1}^{p} \sum_{\alpha_s=1}^{n_s} \frac{R_s e^{-i\phi_s} e^{-2\pi i \alpha_s/n_s}}{1 - X R_s e^{i\phi_s} e^{2\pi i \alpha_s/n_s}}$$
$$= \sum_{s=1}^{p} R_s^2 \sum_{\alpha_s=1}^{n_s} \left(\frac{1}{R_s e^{i\phi_s} e^{2\pi i \alpha_s/n_s}} + \frac{X}{1 - X R_s e^{i\phi_s} e^{2\pi i \alpha_s/n_s}} \right),$$

or

$$\mu(X) = X \sum_{s=1}^{p} R_s^2 \nu_{n_s}(X; R_s e^{i\phi_s}). \tag{18c}$$

We can now work out both sides of Eq. (11). We first note that

$$\nu_n'(X;\zeta) = \frac{n^2 (X\zeta)^n}{X[1-(X\zeta)^n]^2} = \frac{\nu_n^2(X;\zeta) - n\nu_n(X;\zeta)}{X},$$

or

$$X\nu_n' = \nu_n(\nu_n - n). \tag{19}$$

Thus, in (11) we have

$$\nu^2 - X\nu' - \nu = \sum_{s,r=1}^{p} \nu_{n_s}\nu_{n_r} - X\sum_{s=1}^{p} \nu_{n_s}' - \sum_{s=1}^{p} \nu_{n_s}$$
$$= \sum_{s,r=1}^{p} \nu_{n_s}\nu_{n_r} - \sum_{s=1}^{p} (\nu_{n_s}^2 - n_s \nu_{n_s}) - \sum_{s=1}^{p} \nu_{n_s}$$
$$= \sum_{s,r=1}^{p}{}' \nu_{n_s}\nu_{n_r} + \sum_{s=1}^{p} (n_s - 1)\nu_{n_s},$$

where the prime on the double sum means $s \neq r$. Thus,

$$\sum_{s=1}^{p} (2R_s^2 - n_s + 1)\nu_{n_s} = \sum_{s,r=1}^{p}{}' \nu_{n_s}\nu_{n_r}. \tag{20}$$

This is our basic result that we now specialize to various cases.

A. Two nested polygons

Consider the simplest case $p=2$. Clearing the denominators we get from (20)

$$n_1(2R_1^2 - n_1 + 1)[1 - (XR_2 e^{i\phi_2})^{n_2}]$$
$$+ n_2(2R_2^2 - n_2 + 1)[1 - (XR_1 e^{i\phi_1})^{n_1}] = 2n_1 n_2.$$

If $n_1 \neq n_2$, the coefficients of X^{n_1} and X^{n_2} must vanish separately. This would require

$$2R_1^2 = n_1 - 1$$

and

$$2R_2^2 = n_2 - 1.$$

But the constant term,

$$n_1(2R_1^2 - n_1 + 1) + n_2(2R_2^2 - n_2 + 1) - 2n_1 n_2,$$

must also vanish, and if R_1 and R_2 have the values just indicated, this would imply that $n_1 n_2$ vanishes, which is unacceptable.

We conclude that $n_1 = n_2 = n$ in order to have a solution, and then that

$$(2R_1^2 - n + 1)[1 - (XR_2 e^{i\phi_2})^n]$$
$$+ (2R_2^2 - n + 1)[1 - (XR_1 e^{i\phi_1})^n] = 2n.$$

Equating the constant term and the coefficient of X^n to zero we obtain

$$R_1^2 + R_2^2 = 2n - 1, \tag{21a}$$

$$(2R_2^2 - n + 1)(R_1 e^{i\phi_1})^n + (2R_1^2 - n + 1)(R_2 e^{i\phi_2})^n = 0. \tag{21b}$$

The second of these may be written

$$(2R_2^2 - n + 1)R_1^n e^{in(\phi_1 - \phi_2)} + (2R_1^2 - n + 1)R_2^n = 0,$$

from which we conclude that the exponential must be real, i.e., equal to ± 1. These two possibilities correspond to the polygons being symmetrically arranged, with the vortices both on the same spokes from the center, or in a staggered arrangement, with the vortices in one polygon rotated by π/n relative to those in the other. For the symmetrical case we get using (21a),

$$(2R_1^2 - 3n + 1)R_1^n + (2R_2^2 - 3n + 1)R_2^n = 0. \tag{22a}$$

For the staggered case we have

$$(2R_1^2 - 3n + 1)R_1^n - (2R_2^2 - 3n + 1)R_2^n = 0. \tag{22b}$$

If we set $\xi = R_1/R_2$, we may recast (21a) and (22) as a single equation for ξ,

$$R_2^2(1 + \xi^2) = 2n - 1,$$

$$(2R_2^2\xi^2 - 3n + 1)\xi^n \pm (2R_2^2 - 3n + 1) = 0,$$

so

$$\left(2\frac{2n-1}{1+\xi^2}\xi^2 - 3n + 1\right)\xi^n \pm \left(2\frac{2n-1}{1+\xi^2} - 3n + 1\right) = 0,$$

or

$$(n-1)\xi^{n+2} - (3n-1)\xi^n - (3n-1)\xi^2 + (n-1) = 0 \tag{23a}$$

for the symmetrical case and

$$(n-1)\xi^{n+2} - (3n-1)\xi^n + (3n-1)\xi^2 - (n-1) = 0 \tag{23b}$$

for the staggered case. These results are in accord with previously published results on "double rings" obtained directly from the equations of motion.[1,5]

B. Three nested polygons

Let us now consider the case of three nested, regular polygons. Returning to (20) and clearing the denominators, we obtain

$$n_1(2R_1^2 - n_1 + 1)[1 - (XR_2e^{i\phi_2})^{n_2}][1 - (XR_3e^{i\phi_3})^{n_3}]$$
$$+ n_2(2R_2^2 - n_2 + 1)[1 - (XR_3e^{i\phi_3})^{n_3}][1 - (XR_1e^{i\phi_1})^{n_1}]$$
$$+ n_3(2R_3^2 - n_3 + 1)[1 - (XR_1e^{i\phi_1})^{n_1}][1 - (XR_2e^{i\phi_2})^{n_2}]$$
$$= 2n_1n_2[1 - (XR_3e^{i\phi_3})^{n_3}] + 2n_2n_3[1 - (XR_1e^{i\phi_1})^{n_1}]$$
$$+ 2n_3n_1[1 - (XR_2e^{i\phi_2})^{n_2}]. \quad (24)$$

Balancing the terms independent of X gives the obvious relation

$$n_1R_1^2 + n_2R_2^2 + n_3R_3^2 = \tfrac{1}{2}N(N-1), \quad (25)$$

where

$$N = n_1 + n_2 + n_3.$$

Now, let us first assume that $n_1 < n_2 < n_3$. Then the highest-order term in X is the term in $X^{n_2+n_3}$, i.e., we must have

$$2R_1^2 = n_1 - 1. \quad (26a)$$

The lowest-order terms in X are the terms in X^{n_1}. Balancing their coefficients gives

$$n_2(2R_2^2 - n_2 + 1) + n_3(2R_3^2 - n_3 + 1) = 2n_2n_3.$$

Combining this with (25) we have

$$2n_1R_1^2 = N(N-1) - 2n_2n_3 - n_2(n_2-1) - n_3(n_3-1)$$

or

$$2n_1R_1^2 = N(N-1) - (n_2+n_3)^2 + n_2 + n_3$$
$$= N(N-1) - (N-n_1)^2 + N - n_1,$$

i.e.,

$$2R_1^2 = 2N - n_1 - 1. \quad (26b)$$

But (26a) and (26b) taken together give $n_1 = N$, which is unacceptable. Thus, two of the polygons must have the same number of vertices.

Let the indexing be chosen such that $n_1 = n_2 = n$. Equation (24) now has terms of degree 0, n, $2n$, n_3, and n_3+n. Let us assume that $n_3 \neq n$ and $n_3 \neq 2n$, such that the terms in (24) of degree n_3 have to balance individually. Then we get

$$R_1^2 + R_2^2 = 2n - 1.$$

Similarly, since there is just one term of degree $2n$, its coefficient must vanish, i.e.,

$$2R_3^2 = n_3 - 1.$$

But these two results are incompatible with (25). We conclude, therefore, that we must either have $n_3 = n$ or $n_3 = 2n$.

For $n_3 = 2n$ Eqs. (24) take the form

$$(2R_1^2 - n + 1)[1 - (XR_2e^{i\phi_2})^n][1 - (XR_3e^{i\phi_3})^{2n}]$$
$$+ (2R_2^2 - n + 1)[1 - (XR_3e^{i\phi_3})^{2n}][1 - (XR_1e^{i\phi_1})^n]$$
$$+ 2(2R_3^2 - 2n + 1)[1 - (XR_1e^{i\phi_1})^n][1 - (XR_2e^{i\phi_2})^n]$$
$$= 2n[1 - (XR_3e^{i\phi_3})^{2n}] + 4n[1 - (XR_1e^{i\phi_1})^n]$$
$$+ 4n[1 - (XR_2e^{i\phi_2})^n]. \quad (27)$$

The coefficient relations are (for the constant term, and the terms of degree n, $2n$, and $3n$, respectively)

$$R_1^2 + R_2^2 + 2R_3^2 = 8n - 2, \quad (28a)$$

$$(2R_1^2 + 4R_3^2 - 9n + 3)(R_2e^{i\phi_2})^n + (2R_2^2 + 4R_3^2 - 9n + 3)$$
$$\times (R_1e^{i\phi_1})^n = 0, \quad (28b)$$

$$(R_1^2 + R_2^2 - 2n + 1)(R_3e^{i\phi_3})^{2n} = (2R_3^2 - 2n + 1)$$
$$\times (R_1e^{i\phi_1})^n(R_2e^{i\phi_2})^n, \quad (28c)$$

$$(2R_1^2 - n + 1)(R_2e^{i\phi_2})^n + (2R_2^2 - n + 1)(R_1e^{i\phi_1})^n = 0. \quad (28d)$$

If we use (28a) in (28b) and (28c) we obtain the equations

$$(2R_1^2 - 7n + 1)(R_1e^{i\phi_1})^n + (2R_2^2 - 7n + 1)(R_2e^{i\phi_2})^n = 0, \quad (28b')$$

$$(2R_3^2 - 2n + 1)(R_1e^{i\phi_1})^n(R_2e^{i\phi_2})^n + (2R_3^2 - 6n + 1)$$
$$\times (R_3e^{i\phi_3})^{2n} = 0. \quad (28c')$$

Taken together (28d) and (28b′) show that $\exp\{i(\phi_1 - \phi_2)n\}$ must be real, i.e., $= \pm 1$. We thus have

$$(2R_1^2 - 7n + 1)R_1^n \pm (2R_2^2 - 7n + 1)R_2^n = 0, \quad (28b'')$$

$$(2R_2^2 - n + 1)R_1^n \pm (2R_1^2 - n + 1)R_2^n = 0. \quad (28d')$$

Adding these and using (28a) again, we get

$$(4R_3^2 - 8n + 2)(R_1^n \pm R_2^n) = 0.$$

Thus, when the + sign is used, i.e., for the symmetric configuration of these two polygons, we must have

$$2R_3^2 = 4n - 1. \quad (29)$$

When the − sign is used, i.e., for the staggered configuration, we may also have $R_1 = R_2$. We now show that in all cases we are led to $R_1 = R_2$. If (29) holds, then in (28c′) we have simply

$$(R_3e^{i\phi_3})^{2n} = (R_1e^{i\phi_1})^n(R_2e^{i\phi_2})^n,$$

which implies

$$R_3^2 = R_1R_2.$$

But then by (28a) and (29)

$$(R_1 - R_2)^2 = R_1^2 + R_2^2 - 2R_3^2 = 0,$$

or $R_1 = R_2$. Therefore, the case $n_3 = 2n$ reduces to two nested polygons and has already been covered in our analysis in Sec. VI A.

The only new cases of three nested polygons, then, are for $n_3 = n$. Equation (24) now becomes

$$(2R_1^2 - n + 1)[1 - (XR_2e^{i\phi_2})^n][1 - (XR_3e^{i\phi_3})^n]$$
$$+ (2R_2^2 - n + 1)[1 - (XR_3e^{i\phi_3})^n][1 - (XR_1e^{i\phi_1})^n]$$
$$+ (2R_3^2 - n + 1)[1 - (XR_1e^{i\phi_1})^n][1 - (XR_2e^{i\phi_2})^n]$$

$$= 2n[1-(XR_1e^{i\phi_1})^n] + 2n[1-(XR_2e^{i\phi_2})^n] + 2n[1-(XR_3e^{i\phi_3})^n]. \tag{30}$$

This leads to the following coefficient relations for the terms of order 0, n, and $2n$ in X:

$$2R_1^2 + 2R_2^2 + 2R_3^2 = 9n - 3, \tag{31a}$$

$$(2R_2^2 + 2R_3^2 - 4n + 2)(R_1e^{i\phi_1})^n + (2R_3^2 + 2R_1^2 - 4n + 2) \times (R_2e^{i\phi_2})^n + (2R_1^2 + 2R_2^2 - 4n + 2)(R_3e^{i\phi_3})^n = 0, \tag{31b}$$

$$(2R_1^2 - n + 1)(R_2e^{i\phi_2})^n(R_3e^{i\phi_3})^n + (2R_2^2 - n + 1) \times (R_3e^{i\phi_3})^n(R_1e^{i\phi_1})^n + (2R_3^2 - n + 1) \times (R_1e^{i\phi_1})^n(R_2e^{i\phi_2})^n = 0. \tag{31c}$$

We can use (31a) to simplify (31b) somewhat

$$(2R_1^2 - 5n + 1)(R_1e^{i\phi_1})^n + (2R_2^2 - 5n + 1)(R_2e^{i\phi_2})^n + (2R_3^2 - 5n + 1)(R_3e^{i\phi_3})^n = 0. \tag{31b′}$$

This equation has the form

$$f(R_1)e^{in\phi_1} + f(R_2)e^{in\phi_2} + f(R_3)e^{in\phi_3} = 0,$$

where

$$f(R) = (2R^2 - 5n + 1)R^n. \tag{31d}$$

We can recast (31c) in this form as well,

$$g(R_1)e^{in\phi_1} + g(R_2)e^{in\phi_2} + g(R_3)e^{in\phi_3} = 0, \tag{31c′}$$

where

$$g(R) = \frac{2R^2 - n + 1}{R^n}. \tag{31e}$$

We think of (31b′) and (31c′) as saying that the scalar products of the "phase vector,"

$$(e^{in\phi_1}, e^{in\phi_2}, e^{in\phi_3})$$

and two different "vectors," (f_1, f_2, f_3) and (g_1, g_2, g_3), where $f_1 = f(R_1)$, $g_1 = g(R_1)$, etc., with real components both vanish. It follows that the phase vector itself is proportional to the "vector product" of these two real vectors. While the coefficient of proportionality may be complex, the ratio of any two components of the phase vector must be real. In other words, the phase factors,

$$e^{in(\phi_1-\phi_2)}, \quad e^{in(\phi_2-\phi_3)}, \quad e^{in(\phi_3-\phi_1)},$$

are all real, and hence all $=\pm 1$. The nested polygons are, therefore, arranged either symmetrically or staggered with respect to one another.

We analyze this general case in considerable detail below. However, we must subsequently return to the one major exception when the two aforementioned real vectors are parallel. We call this the "degenerate case" and provide an analysis of the equilibria to which it gives rise in Sec. VI D.

There are, essentially, only two possibilities in the general case: (i) all three polygons are symmetrically arranged with respect to one another; (ii) two are symmetrically arranged, and the third is staggered relative to these two.

Thus, the system of equations to be solved for the radii is either

$$2R_1^2 + 2R_2^2 + 2R_3^2 = 9n - 3, \tag{32}$$

along with

$$(2R_1^2 - 5n + 1)R_1^n + (2R_2^2 - 5n + 1)R_2^n + (2R_3^2 - 5n + 1)R_3^n = 0, \tag{33a}$$

$$\frac{2R_1^2 - n + 1}{R_1^n} + \frac{2R_2^2 - n + 1}{R_2^n} + \frac{2R_3^2 - n + 1}{R_3^n} = 0, \tag{33b}$$

for the symmetrical case (i), or (32) along with

$$(2R_1^2 - 5n + 1)R_1^n + (2R_2^2 - 5n + 1)R_2^n - (2R_3^2 - 5n + 1)R_3^n = 0, \tag{34a}$$

$$\frac{2R_1^2 - n + 1}{R_1^n} + \frac{2R_2^2 - n + 1}{R_2^n} - \frac{2R_3^2 - n + 1}{R_3^n} = 0, \tag{34b}$$

for the staggered case (ii), where we have assumed the indexing is such that the two polygons that are symmetrically arranged are 1 and 2, and the staggered polygon is 3.

The simplest case, $n=2$ in the symmetric configuration, provides an interesting check on these developments. In this case Eqs. (32) and (33) become

$$R_1^2 + R_2^2 + R_3^2 = \tfrac{15}{2},$$

$$R_1^4 + R_2^4 + R_3^4 = \tfrac{135}{4},$$

$$\frac{1}{R_1^2} + \frac{1}{R_2^2} + \frac{1}{R_3^2} = 6.$$

Thus,

$$(R_1^2 + R_2^2 + R_3^2)^2 = \tfrac{225}{4} = R_1^4 + R_2^4 + R_3^4 + 2(R_1^2R_2^2 + R_2^2R_3^2 + R_3^2R_1^2)$$

or

$$R_1^2R_2^2 + R_2^2R_3^2 + R_3^2R_1^2 = \tfrac{45}{4}.$$

Then, from

$$\frac{R_1^2R_2^2 + R_2^2R_3^2 + R_3^2R_1^2}{R_1^2R_2^2R_3^2} = 6,$$

we get

$$R_1^2R_2^2R_3^2 = \tfrac{15}{8}.$$

In this special case the vortices are located on a line, which we take to be the x axis, at $x = \pm R_1, \pm R_2, \pm R_3$. Thus, the polynomial

$$P(x) = (x - z_1)\cdots(x - z_6) = (x^2 - R_1^2)(x^2 - R_2^2)(x^2 - R_3^2) = x^6 - \tfrac{15}{2}x^4 + \tfrac{45}{4}x^2 - \tfrac{15}{8}.$$

But this is just H_6, the Hermite polynomial of degree 6 (divided by 64), as we know independently that it must be.[1]

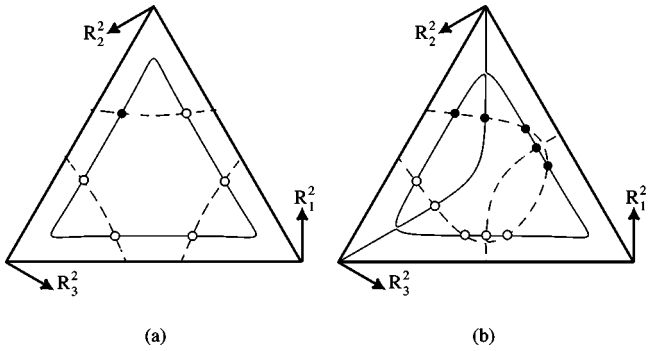

FIG. 1. Trilinear coordinate plots for $n=9$ based on (32) for (a) the symmetric case [Eqs. (33a) and (33b)] and (b) the staggered case [Eqs. (34a) and (34b)]. The physically distinct configurations are indicated by solid dots; the open dots give solutions that arise from these by permutation of indices 1, 2, and 3.

C. Geometrical solution

Solving Eqs. (32)–(34) for general n algebraically appears complicated, not to say impossible. However, we may obtain a concise overview of the solution space by the following geometrical device: Let R_1^2, R_2^2, and R_3^2 be represented as trilinear coordinates. Then Eq. (32) can be "built into" the representation by letting the height of the basic equilateral triangle in this coordinate system equals $(9n-3)/2$ (see Ref. 10 for a general discussion of trilinear coordinates and their uses in fluid mechanics). Equations (33a) and (33b) or (34a) and (34b) now represent two sets of auxiliary curves, one for the symmetric case and one for the staggered case, that can be plotted in the trilinear diagram. The points of intersection of these curves, two and two, define the solutions of the problem of equilibria for nested n-gons.

Figure 1 shows these trilinear plots when $n=9$ for (a) the symmetric and (b) the staggered cases. The three axes in the trilinear coordinate system are indicated. The curves corresponding to Eqs. (33a) and (34a) are shown as dashed lines. The curves corresponding to Eqs. (33b) and (34b) are shown as solid lines. The points of intersection are marked either by solid or open dots. The solid dots give a set of intersections that correspond to physically different equilibria. The open dots show the additional equilibria that arise from relabeling the three radii. For the symmetric case we may freely interchange any of the three indices 1, 2, and 3. For the staggered case only transposition of 1 and 2 is permitted. Thus, from Fig. 1(a) we see that there is just one equilibrium configuration for three symmetrically nested regular nine-gons, whereas Fig. 1(b) shows that there are five different equilibria for three regular nine-gons when two are symmetrically nested and one is staggered.

The curve (33a) intersects the sides of the equilateral triangle in six points. (We discuss the intersections of (34a) and the trilinear coordinate axes below.) For example, the points of intersection with the R_1 axis are given by setting $R_1=0$ in (32) and (33a), viz.,

$$R_2^2 + R_3^2 = \frac{9n-3}{2},$$

TABLE I. Radii of symmetrically nested n-gons; units according to Eqs. (32) and (34). If an illustration is provided, the figure panel number is noted.

n	R_1	R_2	R_3	Illustration
2	2.350 604 973 7	0.436 077 411 9	1.335 849 074 0	Fig. 4(a)
3	2.845 615 597 9	0.801 944 921 8	1.805 368 719 0	Fig. 4(b)
4	3.250 362 127 7	1.088 190 194 7	2.179 676 154 7	Fig. 4(c)
5	3.604 522 111 4	1.323 069 827 2	2.501 380 934 8	Fig. 4(d)
6	3.925 078 030 8	1.522 050 411 2	2.788 749 719 5	Fig. 4(e)
7	4.221 020 895 1	1.694 752 937 7	3.051 359 546 6	
8	4.497 760 084 7	1.847 818 793 9	3.294 801 955 3	
9	4.758 869 438 0	1.986 059 846 3	3.522 602 441 2	Fig. 2(a)
25	7.876 461 953 1	3.464 098 790 9	6.079 586 060 5	Fig. 4(f)

$$(2R_2^2 - 5n + 1)R_2^n + (2R_3^2 - 5n + 1)R_3^n = 0.$$

These equations are reminiscent of (21a) and (22a). Indeed, they yield the radii for a centered two-ring equilibrium in which there is a vortex of circulation $n\Gamma$ at the center of two symmetric n-gons, each with vortices of circulation Γ at its vertices. Introducing $\chi=R_2/R_3$ we find the following equation for χ [cf. the reduction of (21a) and (22a) to (23a)]:

$$(4n-2)\chi^{n+2} - (5n-1)\chi^n - (5n-1)\chi^2 + (4n-2) = 0. \tag{35}$$

From the diagrams it appears that there are two solutions to this equation.

It is not difficult to construct the actual equilibria from the data in Fig. 1. Newton's method readily gives the values of the radii (see Tables I and II) and the arrangement around the three circles is known. Figure 2 provides pictures of the six different equilibrium patterns for identical vortices ar-

TABLE II. Radii of nested n-gons, two (indices 1 and 2) symmetrically arranged and one staggered (index 3); units according to Eqs. (32) and (34b). The figure panel in which the vortex configuration is illustrated is given.

n	R_1	R_2	R_3	Illustration
2	0.696 117 752 5	1.973 444 400 9	1.766 617 466 0	Fig. 6(a)
3	1.007 204 248 1	2.427 970 523 5	2.256 213 363 1	Fig. 6(b)
4	1.231 786 477 4	2.800 492 298 2	2.672 067 544 4	Fig. 6(c)
5	1.418 509 932 7	3.129 852 520 8	3.031 806 848 8	Fig. 6(d)
6	1.583 669 110 6	3.432 476 716 9	3.348 148 105 4	Fig. 6(e)
6	2.428 847 677 7	3.834 088 405 7	2.213 699 405 0	Fig. 6(f)
6	2.719 074 979 6	3.903 123 555 5	1.694 773 662 1	Fig. 6(g)
7	1.734 056 952 1	3.725 948 373 0	3.620 822 449 2	Fig. 6(h)
7	2.593 407 316 3	4.133 252 285 2	2.488 064 315 6	Fig. 6(i)
7	3.013 185 669 4	4.210 379 067 0	1.787 014 335 1	Fig. 6(j)
8	1.875 519 206 6	4.126 462 929 7	3.735 603 217 1	Fig. 6(k)
8	2.763 142 438 6	4.419 917 607 2	2.707 281 331 7	Fig. 6(l)
8	3.272 461 184 8	4.492 304 839 5	1.900 051 321 1	Fig. 6(m)
9	4.756 040 998 1	3.509 292 661 7	2.016 169 397 3	Fig. 2(b)
9	4.692 035 445 5	2.929 526 510 2	2.898 737 277 7	Fig. 2(c)
9	4.508 864 315 0	2.005 129 229 1	3.827 479 505 3	Fig. 2(d)
9	4.174 380 729 7	1.999 879 463 0	4.192 258 061 8	Fig. 2(e)
9	3.846 738 493 4	1.995 360 456 8	4.496 792 146 7	Fig. 2(f)

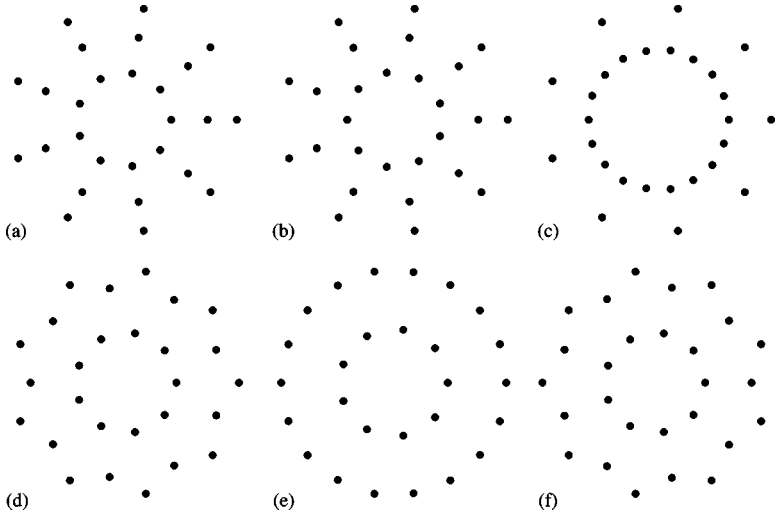

FIG. 2. The six possible equilibrium patterns for three nested, regular nine-gons of identical vortices (a) the single symmetric pattern; (b)–(f) the five staggered patterns. [These correspond to the solid dots in Fig. 1(b) starting from the left and moving clockwise.]

ranged in regular nine-gons on three nested circles. The five staggered patterns are displayed in Fig. 2 such that they correspond to the points of intersection shown as solid dots in Fig. 1 starting at the left-hand border and working clockwise along the curve (34a).

The diagrams for the symmetrically arranged case do not change substantially with n. In Fig. 3 we show such diagrams for $n=2$, 3, 4, 5, 6, and 25. Thus, we conclude that for any n there is just *one* symmetric arrangement of three nested, regular n-gons of identical vortices.

For large n the nature of the diagram is that (33a) and (33b) both approximately are equilateral triangles with (33b) having sides parallel to the coordinate axes in the trilinear coordinate system, and (33a) being turned "upside down." The values of the intersection points are

$$2R_1^2 \approx 5n-1, \quad 2R_2^2 \approx 3n-1, \quad 2R_3^2 \approx n-1, \tag{36}$$

and permutations thereof. For $n=9$ numerical solution of Eqs. (32), (33a), and (33b) (cf. Table I) gives

$$R_1 = 4.76\ldots, \quad R_2 = 3.52\ldots, \quad R_3 = 1.99\ldots,$$

whereas the approximation (36) gives the values

$$R_1 = 4.69\ldots, \quad R_2 = 3.61\ldots, \quad R_3 = 2.0.$$

In Table I we have collected the numerical values of the three radii for $n=2,\ldots,9$ and for $n=25$. In Fig. 4 we show the actual configurations of the vortices corresponding to the panels in Fig. 3.

The staggered configurations offer a richer picture. Repeating the construction in Fig. 1(b) for $n=2$, 3,…, 8 and 25 yields the diagrams in Fig. 5. (The diagram for $n=15$ appears in Fig. 7.) In each diagram the solid curve corresponds to Eq. (34b), and the dashed curve to Eq. (34a). We see that the portion of the curve (34b) that passes through a vertex of the equilateral triangle asymptotes to one of the lines $R_1=R_3$ or $R_2=R_3$. For all diagrams in Fig. 5, except the last one, the intersections of (34a) with the R_1 and R_2 axes occur at $R_2=R_3$ and $R_1=R_3$, respectively. Thus, the corresponding centered equilibria consist of one vortex of circulation $n\Gamma$ at the origin surrounded by a regular $2n$-gon, i.e., the two staggered n-gons of the same size form a regular $2n$-gon. [The intersections of the curve (34a) with the R_3 axis are, of course, the same points we found for the symmetric case above.] For $n=25$, however, there are three points of intersection with both the R_1 and the R_2 axes. Thus, for sufficiently large n

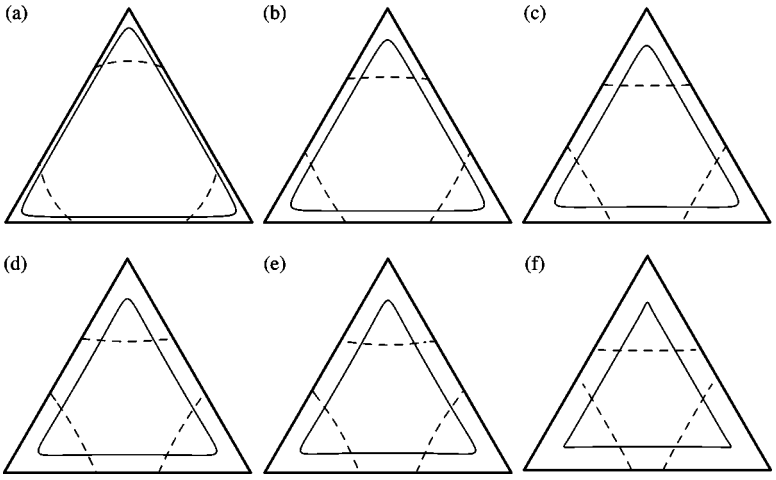

FIG. 3. Trilinear coordinate plots for the symmetric case of three nested n-gons when (a) $n=2$, (b) 3, (c) 4, (d) 5, (e) 6, and (f) 25. The diagram for $n=9$ was given in Fig. 1(a). The diagrams are very similar and lead to the conclusion that there is just one symmetric configuration.

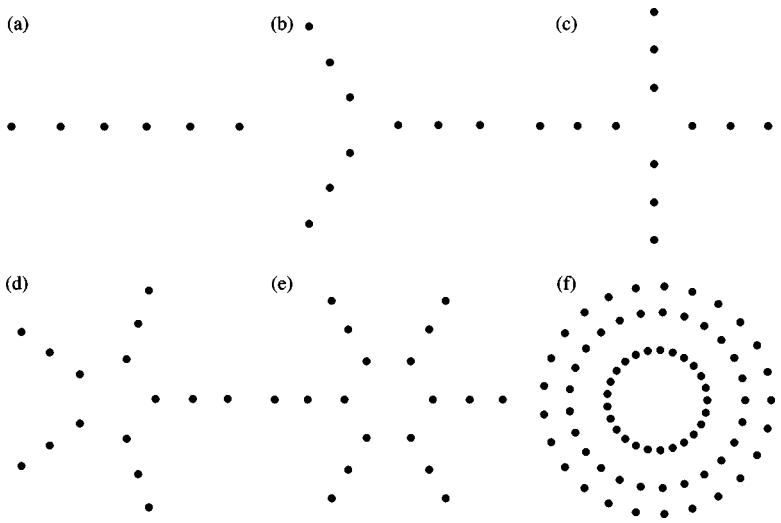

FIG. 4. Equilibrium patterns of three nested, regular n-gons arranged symmetrically for (a) $n=2$, (b) 3, (c) 4, (d) 5, (e) 6, and (f) 25.

there must exist equilibria with a vortex of strength $n\Gamma$ at the center surrounded by two staggered n-gons. Closer analysis shows that these equilibria arise only for $n \geqslant 17$. (Figure 7 shows that this equilibrium does not exist for $n=15$.)

In general the number of intersections of the two curves (34a) and (34b) within the equilateral triangle (points outside correspond to negative values of R_1, R_2, or R_3 and, thus, are unphysical) is determined to sufficient accuracy from the numerically generated plots and may be counted in the various panels of the diagram. In this way we find the following number of essentially different staggered configurations of three nested n-gons: For $n=2$, 3, 4, and 5 we have one configuration; for $n=6$, 7, and 8 we have three; and for $n \geqslant 9$ we have five. The only two issues that need further analysis/examination are (i) the case $n=8$ where the plot in Fig. 5(g) suggests two points of common tangency between (34a) and (34b), and (ii) the asymptotic result that there are five configurations for all $n \geqslant 9$.

The issue of whether (34a) and (34b) have a common point of tangency is resolved most simply by performing a high-resolution plot of the two curves close to the apparent point of common tangency. This shows unequivocally that, although the two curves do come very close, there is no common point. Thus, for $n=8$ there are just three solutions.

The asymptotic result (ii) follows, at least heuristically, by noting that for large n the curve (34b) must largely consist of portions for which either $R_1=R_3$, $R_2=R_3$, or the smallest of R_1, R_2, and R_3 is "pinned down" to the value $\sqrt{[(n-1)/2]}$. What this means for the curve (34b) is quite evident in the panel Fig. 5(h) for $n=25$. Similarly, the curve (34a) for large n must consist of portions for which either $R_1=R_3$, $R_2=R_3$, or the largest of R_1, R_2, and R_3 is $\sqrt{[(5n-1)/2]}$. Again, this is quite obvious from Fig. 5(h). The center of the equilateral triangle is, of course, a "forbidden" point since it corresponds to $R_1=R_2$, i.e., would lead to the overlap of vortices.

Table II provides numerically computed results for the three radii for $n=2,\ldots, 9$ (the allowed permutations of indices 1 and 2 are not listed). In Fig. 6 we have plotted the 13 configurations given by the data in Table II for $2 \leqslant n \leqslant 8$. [Figures 2(b)–2(f) gave the configurations for $n=9$.] Several of these equilibria superficially have the appearance of two-ring configurations with twice as many vortices in one ring as in the other [cf. Figs. 2(c) and 2(e); Figs. 6(b)–6(d), 6(h), 6(i), and 6(l)]. Table II shows that, indeed, even for these smaller values of n, where the asymptotic approximation cannot be expected to hold with much accuracy, one solution

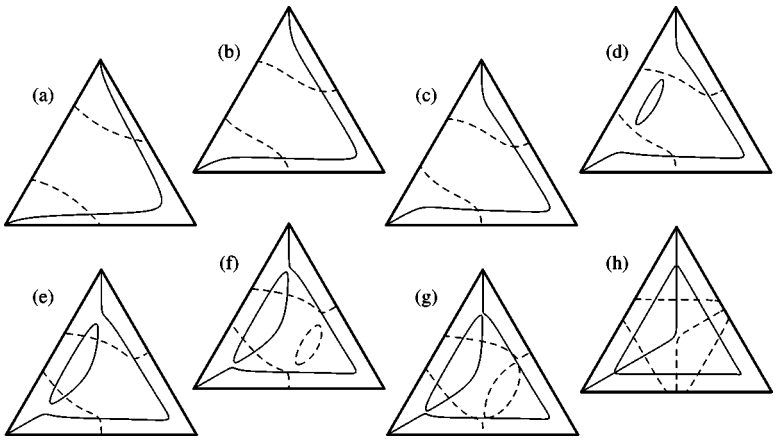

FIG. 5. Trilinear diagram plots for the staggered case of three nested n-gons when (a) $n=2$, (b) 3, (c) 4, (d) 5, (e) 6, (f) 7, (g) 8, and (h) 25. The diagram for $n=9$ was given in Fig. 1(b). The number of intersection points increases from one for $n=2$, 3, 4, and 5, to three for $n=6$, 7, 8, and to five for $n \geqslant 9$.

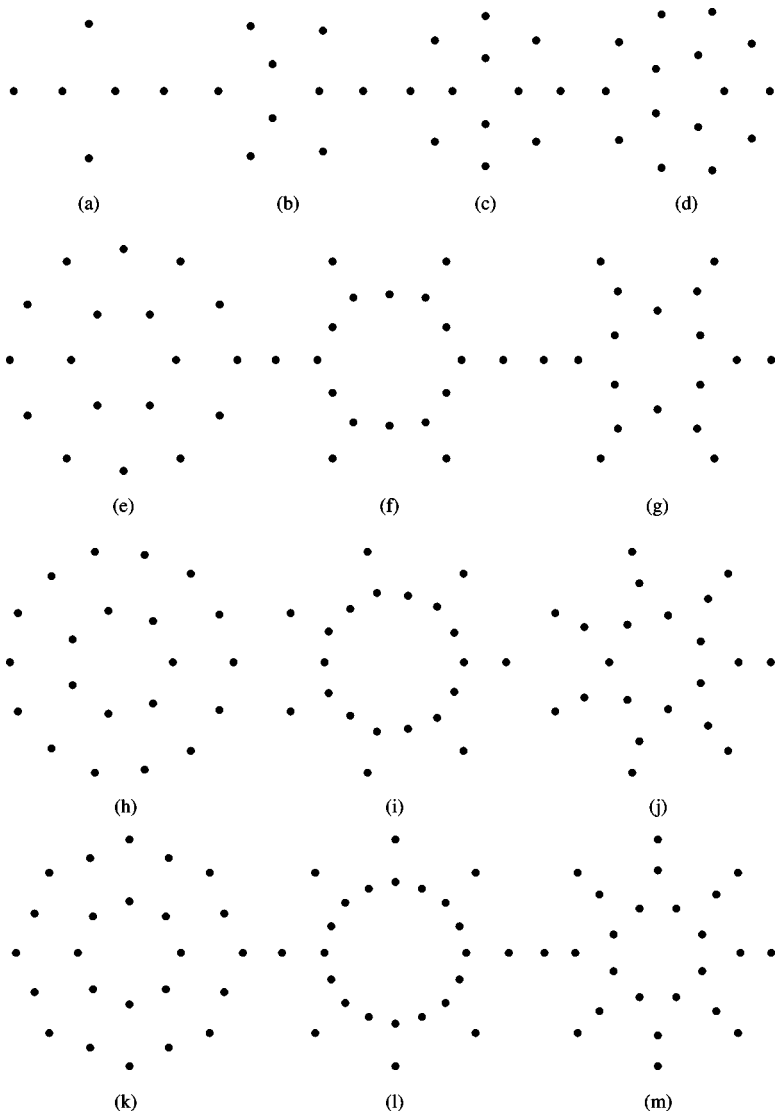

FIG. 6. The unique staggered triple-ring equilibria for (a) $n=2$ (first reported in Aref and Vainchtein, 1998); (b) $n=3$, (c) 4, and (d) 5. The three possibilities for (e–g) $n=6$, (h–j) 7, and (k–m) 8.

usually has either $R_1 \approx R_3$ or $R_2 \approx R_3$. From our earlier work we know that a two-ring equilibrium consisting of a regular n-gon and a regular $2n$-gon is impossible.

The diagram for $n=25$ in Fig. 5(h) gives, in effect, an asymptotic, approximate solution to the problem of vortex triple rings for large n. Consider Fig. 7 where we have shown the diagram corresponding to those in Fig. 5 for $n=15$. We have indicated the five points of intersection of (34a) and (34b) that yield physically distinct equilibria denoted as A, B, C, D, and E. The radii for these five equilibria are given by the following approximations:

$$A: \quad R_1 \approx \sqrt{\frac{5n-1}{2}}, \quad R_2 \approx \sqrt{\frac{3n-1}{2}}, \quad R_3 \approx \sqrt{\frac{n-1}{2}},$$

$$B: \quad R_1 \approx \sqrt{\frac{5n-1}{2}}, \quad R_2 \approx \sqrt{\frac{2n-1}{2}}, \quad R_3 \approx \sqrt{\frac{2n-1}{2}},$$

$$C: \quad R_1 \approx \sqrt{\frac{5n-1}{2}}, \quad R_2 \approx \sqrt{\frac{n-1}{2}}, \quad R_3 \approx \sqrt{\frac{3n-1}{2}},$$

$$D: \quad R_1 \approx \sqrt{\frac{4n-1}{2}}, \quad R_2 \approx \sqrt{\frac{n-1}{2}}, \quad R_3 \approx \sqrt{\frac{4n-1}{2}},$$

$$E: \quad R_1 \approx \sqrt{\frac{3n-1}{2}}, \quad R_2 \approx \sqrt{\frac{n-1}{2}}, \quad R_3 \approx \sqrt{\frac{5n-1}{2}}. \tag{37}$$

To obtain the approximation for point A set the R_1 term of (34a) to zero, the R_3 term of (34b) to zero, and then substitute the results into (32). To obtain the approximation for point B use the same value of R_1 as for point A but now set $R_2=R_3$, and so on. (The approximation A is the one we found in (36) for the single symmetric configuration.)

By way of example, for $n=15$ we have

$$\sqrt{\frac{n-1}{2}} = 2.645\,75\ldots,$$

$$\sqrt{\frac{2n-1}{2}} = 3.807\,89\ldots, \quad \sqrt{\frac{3n-1}{2}} = 4.690\,42\ldots,$$

$$\sqrt{\frac{5n-1}{2}} = 6.082\,76\ldots, \quad \sqrt{\frac{4n-1}{2}} = 5.431\,39\ldots,$$

whereas direct numerical solution of (32), (34a), and (34b) gives the following values for the three radii:

	R_1	R_2	R_3
A:	6.104 677 125 0,	4.661 522 163 2,	2.646 342 442 3,
B:	6.082 769 725 2,	3.808 488 643 1,	3.807 272 872 6,
C:	6.053 083 274 9,	2.646 208 640 6,	4.728 399 591 6,
D:	5.431 358 827 7,	2.645 751 298 5,	5.431 421 669 5,
E:	4.728 999 913 4,	2.645 296 996 7,	6.053 012 772 0.

We show these five equilibria also in Fig. 7.

D. The degenerate case

We return to the special case when the vectors (f_1, f_2, and f_3) and (g_1, g_2, and g_3), see (31d) and (31e), are parallel. In this case we have

$$f_1 g_2 = f_2 g_1, \quad f_2 g_3 = f_3 g_2, \quad f_3 g_1 = f_1 g_3, \tag{38}$$

or

$$(2R_1^2 - 5n + 1)(2R_2^2 - n + 1)R_1^{2n} = (2R_2^2 - 5n + 1)(2R_1^2 - n + 1)R_2^{2n}, \tag{38a}$$

$$(2R_2^2 - 5n + 1)(2R_3^2 - n + 1)R_2^{2n} = (2R_3^2 - 5n + 1)(2R_2^2 - n + 1)R_3^{2n}, \tag{38b}$$

$$(2R_3^2 - 5n + 1)(2R_1^2 - n + 1)R_3^{2n} = (2R_1^2 - 5n + 1)(2R_3^2 - n + 1)R_1^{2n}. \tag{38c}$$

We only need two of these. The third then follows from these two. [The radii in (38) are all >0, and if any term in the parentheses vanishes, all three radii must be equal.] It is easy to plot these three curves in the trilinear coordinate system and to identify the points of intersection. Although it would be sufficient to plot just two of the equations, plotting all three assists in identifying the solutions that arise from one another by permutation of indices.

Once a solution to Eqs. (38a)–(38c) has been found, (31b′) or (31c′) gives

$$f_1 + f_2 e^{in(\phi_2 - \phi_1)} + f_3 e^{in(\phi_3 - \phi_1)} = 0. \tag{39a}$$

From this equation we obtain

$$\cos[n(\phi_2 - \phi_1)] = \frac{f_3^2 - f_2^2 - f_1^2}{2 f_1 f_2}, \qquad \cos[n(\phi_3 - \phi_1)] = -\frac{f_3^2 - f_2^2 + f_1^2}{2 f_1 f_3}. \tag{39b}$$

If the expressions on the right-hand sides are between −1 and 1, we have a solution for the configuration of $3n$ vortices! These limits for both Eqs. (39b) are easily seen to be embodied in the condition $(f_1+f_2+f_3)(-f_1+f_2+f_3)(f_1-f_2+f_3)(f_1+f_2-f_3)=0$. Since the case of a single ring, $R_1=R_2=R_3$, and thus $f_1=f_2=f_3$, is a solution to (38) and (39), albeit an uninteresting one, and since the expression just written is positive for this solution, we may replace (39b) by the simpler criterion

$$(f_1 + f_2 + f_3)(-f_1 + f_2 + f_3)(f_1 - f_2 + f_3)(f_1 + f_2 - f_3) \geqslant 0. \tag{39c}$$

For example, for $n=3$ we produce the trilinear diagram shown in Fig. 8(a). In this diagram we have indicated all the points of intersection described by Eqs. (38a) and (38b). The center of the diagram has all three radii equal and thus all vortices on a circle. We have covered this case above. The three solid dots are the three different solutions—the open dots arise from these by permutation of indices. We note that in this case all solutions have two equal radii. By Newton's method we obtain the following three solutions for the radii:

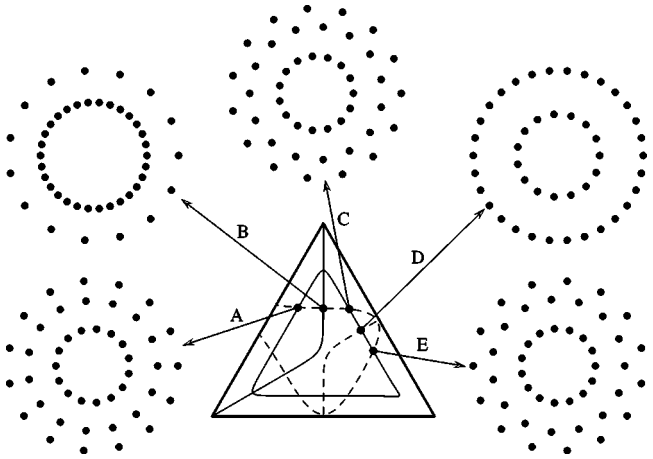

FIG. 7. Graphical analysis for large n, here $n=15$, showing the five intersection points in the trilinear plot and the five equilibria to which they correspond.

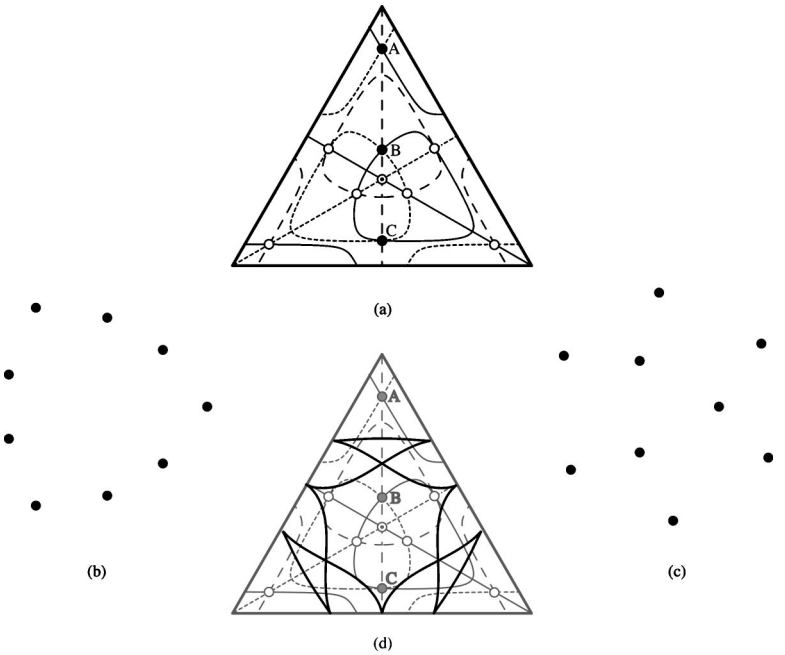

FIG. 8. (a) Trilinear diagram for the "degenerate case" when $n=3$. The three curves (solid, dashed, and dotted) correspond to the three equations (38a)–(38c). The three points of intersections A, B, and C (shown by solid dots) give solutions of Eqs. (38). The open dots correspond to solutions that arise from A, B, and C by permutation of indices. The centered dot corresponds to all vortices being on a single circle. Points B and C correspond to the configurations shown in (b) and (c), respectively. When the angle constraint (39c) is included, panel (d), point A is ruled out.

$$R_1 = 3.167\,603\,205\,9, \quad R_2 = R_3 = 0.991\,536\,668\,5$$
[point A in Fig. 8(a)],

$$R_1 = 2.312\,570\,119\,1, \quad R_2 = R_3 = 1.823\,735\,102\,0$$
[point B in Fig. 8(a)],

$$R_1 = 1.077\,149\,466\,1, \quad R_2 = R_3 = 2.328\,062\,394\,8$$
[point C in Fig. 8(a)].

When the right-hand sides of (39b) are evaluated for these values of the radii, we find that points B and C lead to solutions for the configuration. Point A, however, produces values for the cosine in (39b) that are numerically larger than 1 and so does not lead to a solution. We may also arrive at this conclusion graphically by plotting the boundary curve of the region (39c). This curve is shown in Fig. 8(d) superimposed on the earlier diagram Fig. 8(a). It is clear that points B and C are within the region defined by the inequality (39c). Point A is not. [For $n=2$ all solution points of (38a)–(38c) are disallowed by the angle condition (39c).]

Equations (39b) only produce the angles that rings 2 and 3 are rotated relative to ring 1 up to the ambiguity in the sign of the arccos of the right-hand side. (The addition of 2π times an integer is not an issue, since this simply leads to a change in indexing of the vortices around a given ring.) The only reliable way to decide which sign to use in general would be to return to the basic equations to be solved, Eq. (1), and successively substitute in the finite number of possibilities. In this particular example, since $R_2=R_3$, (39b) simplifies considerably

$$\cos[n(\phi_2-\phi_1)] = \cos[n(\phi_3-\phi_1)] = -\frac{f_1}{2f}, \tag{40a}$$

where f is the common value of f_2 and f_3, and from (39a),

$$\sin[n(\phi_2-\phi_1)] = -\sin[n(\phi_3-\phi_1)]. \tag{40b}$$

It follows from these that

$$\phi_1 = \frac{\phi_2+\phi_3}{2}, \tag{40c}$$

and that we can take either solution of (40a) modulo relabeling of the two rings. In Eq. (40c) we may assume that the coordinates have been rotated such that $\phi_1=0$, so that (40c) signifies that $\phi_3=-\phi_2$. In this way we produce the two configurations shown as (b) and (c) in Fig. 8. The configuration in Fig. 8(c) is one of the few unstable configurations included in the Los Alamos catalog as 9_4.

As we pursue the graphical construction of the solutions of (38a)–(38c) to higher n, we discover that for $n\geqslant 6$ there are solutions of these equations with R_1, R_2, and R_3 all different. However, the condition (39c) rules them all out as three-ring vortex equilibria. Figure 9 shows the trilinear plots for $n=4$, 5, 6, 7, 8, and 9. For $n\geqslant 7$ three "forbidden islands" appear within the diagram due to the angle equation (39c), and the area available for solutions becomes more and more restricted as n increases. We have indicated by small open circles the two available equilibria with $R_2=R_3$. The remaining points of intersection of all three curves are either related to these by symmetry or correspond to a single circle. We conclude, and this may also be argued analytically from (38a)–(38c), that in the degenerate case the only possible solutions have two radii equal for all n.

Let the two equal radii be R_2 and R_3 and let us denote their common value by R. Then we have simply

$$2R_1^2 = 9n - 3 - 4R^2,$$

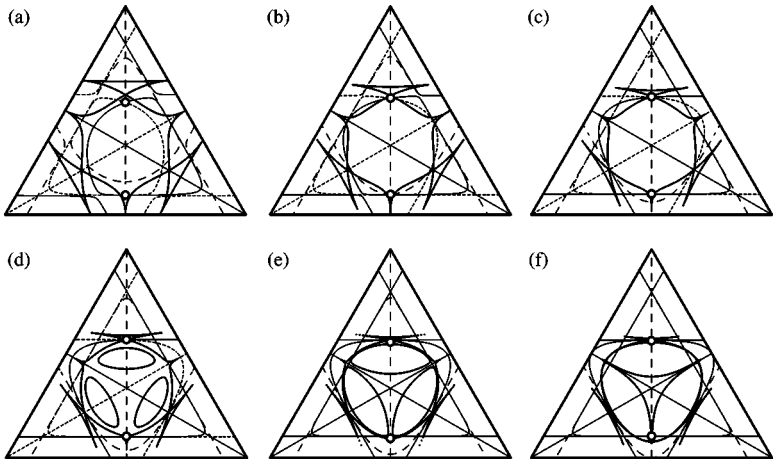

FIG. 9. Trilinear coordinate plots for the "degenerate case" when (a) $n=4$, (b) 5, (c) 6, (d) 7, (e) 8, and (f) 9. Note the key role of the angle constraint (39c), given by the heavier curve, in disqualifying several of the solutions points of Eqs. (38).

$$(2R_1^2 - 5n + 1)(2R^2 - n + 1)R_1^{2n} = (2R^2 - 5n + 1)(2R_1^2 - n + 1)R^{2n}, \tag{32'}$$

as the problem to be solved. From these two equations we obtain the polynomial equation

$$(\rho - 2n + 1)(\rho - n + 1)(9n - 3 - 2\rho)^n = (\rho - 5n + 1)(\rho - 4n + 1)\rho^n, \tag{41}$$

where $\rho = 2R^2$. This equation is of order $n+2$.

One solution of (41) is $\rho = 3n-1$, the value corresponding to the center of the equilateral triangle. Setting $\rho = 2n - 1 + \varepsilon$ we get

$$\varepsilon(n + \varepsilon)(5n - 1 - 2\varepsilon)^n = (3n - \varepsilon)(2n - \varepsilon)(2n - 1 + \varepsilon)^n.$$

For small ε we get to leading order that

$$\varepsilon = \frac{6n}{\left(\frac{5n-1}{2n-1}\right)^n - \frac{6n^2 - 10n + 5}{2n-1}}.$$

For large n this is, indeed, a small quantity. For example, for $n=8$, $\varepsilon \approx 0.02$. Another solution of (41) is therefore quite close to $2n-1$ for large n. Similarly one finds that (41) has solutions close to $n-1$, $4n-1$, and $5n-1$.

Solutions greater than $(9n-3)/2$ are not compatible with (32′). Closer analysis shows that the only solutions of (41) that potentially produce three-ring equilibria are $\rho \approx n - 1, 2n-1$, and $4n-1$. When we include the angle condition (39c), however, the first of these is ruled out and we are left with two configurations for each n which, continuing the tabulation (37), we label

$$F: \quad R_1 \approx \sqrt{\frac{5n-1}{2}}, \quad R_2 = R_3 \approx \sqrt{\frac{2n-1}{2}},$$

$$G: \quad R_1 \approx \sqrt{\frac{n-1}{2}}, \quad R_2 = R_3 \approx \sqrt{\frac{4n-1}{2}}.$$

Already for moderate n the asymptotic R values listed provide excellent approximations to the actual radii. [Note that case F gives 0 for the value of the cosines in (40a) since $f_1 = 0$ for this value of R_1. For the actual solution this value is small but nonzero.]

In Fig. 10 we show the two possible configurations in the "degenerate case" for $n=4$, 5, 6, and 10. There is some similarity between the two-ring configurations F and the prior three-ring configurations B. In the same vein the two-ring configurations G resemble the three-ring configurations

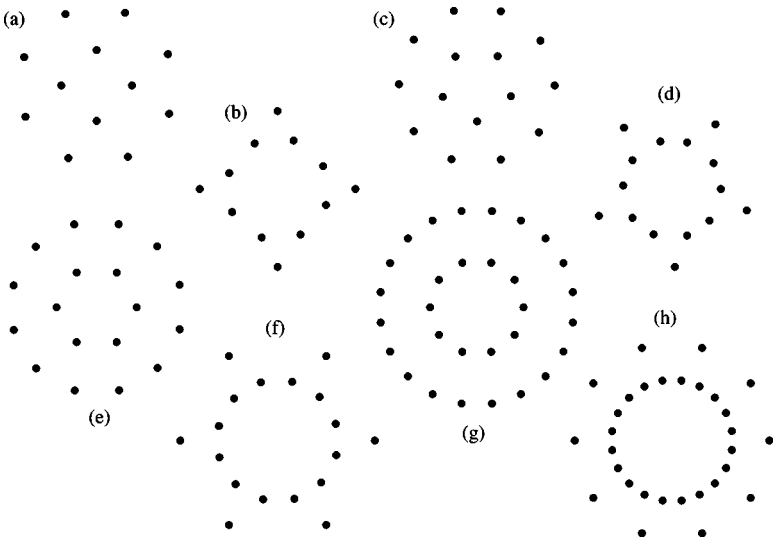

FIG. 10. Equilibria in the "degenerate case" for (a–b) $n=4$, (c–d) 5, (e–f) 6, and (g–h) 10.

D. Interestingly, the equilibrium in Fig. 10(a) is listed as one of the linearly stable equilibria in the Los Alamos catalog (as 12_3) and the state in Fig. 10(c) is listed as the linearly stable 15_2. (On the other hand, the state corresponding to *D* for $n=5$ is listed as the linearly unstable 15_3.) The state in Fig. 10(e) is shown in the Los Alamos catalog as the linearly unstable 18_6.

VII. CENTERED NESTED REGULAR POLYGONS

Let us now return to the developments of Sec. V and consider centered configurations of the type just analyzed, i.e., z_α, $\alpha=1,\ldots,3n=N$ are distributed on three nested, regular *n*-gons, but in addition there is a vortex at the origin for a total of $N+1$ vortices in the configuration.

The derivation in (4′) still holds term by term if we agree to take $N_0=N$. We also obtain (11′) in the same way as in Sec. V. We then get in place of (20)

$$\sum_{s=1}^{p}\frac{n_s(2R_s^2-n_s-1)}{1-(XR_se^{i\phi_s})^{n_s}}=\sum_{s,r=1}^{p}{}'\frac{n_sn_r}{[1-(XR_se^{i\phi_s})^{n_s}][1-(XR_re^{i\phi_r})^{n_r}]}. \tag{20′}$$

A. Two centered, nested polygons

For two centered, nested *n*-gons we have as the counterpart of (21a) and (22a)

$$R_1^2+R_2^2=2n+1, \tag{21a′}$$

$$(2R_1^2-3n-1)R_1^n+(2R_2^2-3n-1)R_2^n=0, \tag{22a′}$$

for the symmetric case, and

$$(2R_1^2-3n-1)R_1^n-(2R_2^2-3n-1)R_2^n=0 \tag{22b′}$$

for the staggered case. With the substitution $\xi=R_1/R_2$ we now get the equation

$$(n+1)\xi^{n+2}-(3n+1)\xi^n-(3n+1)\xi^2+n+1=0,$$

for the symmetrical case, and

$$(n+1)\xi^{n+2}-(3n+1)\xi^n+(3n+1)\xi^2-(n+1)=0,$$

for the staggered case. These results are also known independently.[1]

B. Three centered, nested polygons

For three nested polygons the counterpart of (30) becomes

$$\begin{aligned}&(2R_1^2-n-1)[1-(XR_2e^{i\phi_2})^n][1-(XR_3e^{i\phi_3})^n]\\&\quad+(2R_2^2-n-1)[1-(XR_3e^{i\phi_3})^n][1-(XR_1e^{i\phi_1})^n]\\&\quad+(2R_3^2-n-1)[1-(XR_1e^{i\phi_1})^n][1-(XR_2e^{i\phi_2})^n]\\&\quad=2n[1-(XR_1e^{i\phi_1})^n]+2n[1-(XR_2e^{i\phi_2})^n]\\&\qquad+2n[1-(XR_3e^{i\phi_3})^n].\end{aligned} \tag{30′}$$

The counterpart of (32) then is

$$2R_1^2+2R_2^2+2R_3^2=9n+3, \tag{32″}$$

which is also obvious directly [cf. (5a)]. The counterparts of Eqs. (33) and (34) become

$$(2R_1^2-5n-1)R_1^n+(2R_2^2-5n-1)R_2^n+(2R_3^2-5n-1)R_3^n=0, \tag{33a′}$$

$$\frac{2R_1^2-n-1}{R_1^n}+\frac{2R_2^2-n-1}{R_2^n}+\frac{2R_3^2-n-1}{R_3^n}=0, \tag{33b′}$$

for the symmetric case and

$$(2R_1^2-5n-1)R_1^n+(2R_2^2-5n-1)R_2^n-(2R_3^2-5n-1)R_3^n=0, \tag{34a′}$$

$$\frac{2R_1^2-n-1}{R_1^n}+\frac{2R_2^2-n-1}{R_2^n}-\frac{2R_3^2-n-1}{R_3^n}=0, \tag{34b′}$$

for the staggered case.

We leave it to the reader to verify that the symmetric case for $n=2$ leads to the vortices being situated at the roots of H_7, the seventh Hermite polynomial. This is a well known result.[1]

The analysis proceeds much as in Sec. VI C. The trilinear diagrams can be constructed as before. The height is now $(9n+3)/2$ rather than $(9n-3)/2$. The curves corresponding to the two pairs of Eqs. (33a′), (33b′), (34a′), and (34b′) are qualitatively similar to the curves for the noncentered case. There is one symmetric centered arrangement of three regular *n*-gons. For $n=2$, 3, 4, 5, and 6 there is just one staggered centered configuration of three regular *n*-gons. For $n=7,8$ there are three, and for $n\geqslant 9$ there are five. The asymptotic approximation for these five states is

$$A′:\quad R_1\approx\sqrt{\frac{5n+1}{2}},\quad R_2\approx\sqrt{\frac{3n+1}{2}},\quad R_3\approx\sqrt{\frac{n+1}{2}},$$

$$B′:\quad R_1\approx\sqrt{\frac{5n+1}{2}},\quad R_2\approx\sqrt{\frac{2n+1}{2}},\quad R_3\approx\sqrt{\frac{2n+1}{2}},$$

$$C′:\quad R_1\approx\sqrt{\frac{5n+1}{2}},\quad R_2\approx\sqrt{\frac{n+1}{2}},\quad R_3\approx\sqrt{\frac{3n+1}{2}},$$

$$D′:\quad R_1\approx\sqrt{\frac{4n+1}{2}},\quad R_2\approx\sqrt{\frac{n+1}{2}},\quad R_3\approx\sqrt{\frac{4n+1}{2}},$$

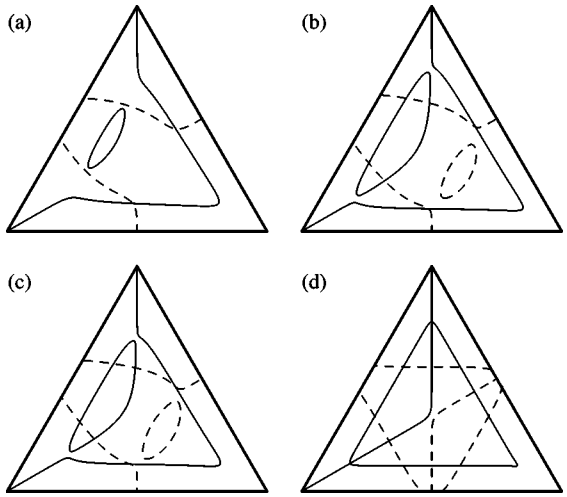

FIG. 11. Trilinear diagram plots for the case of three centered, nested, staggered n-gons when (a) $n=6$, (b) 7, (c) 8, and (d) 25.

$$E': \quad R_1 \approx \sqrt{\frac{3n+1}{2}}, \quad R_2 \approx \sqrt{\frac{n+1}{2}},$$

$$R_3 \approx \sqrt{\frac{5n+1}{2}}. \tag{37'}$$

The centered triple rings look very much like the corresponding noncentered ones—except that there is a vortex at the center. Since there were three noncentered vortex triple rings for $n=6$, one might wonder what the unique centered triple ring looks like. As might have been anticipated, it is the configuration in Fig. 6(e) that is "modified" to accommodate a central vortex. This configuration approximates a circular cutout of a triangular lattice. Figure 11 shows the trilinear diagrams for centered triple rings when $n=6$, 7, 8, and 25. Figure 12 provides examples of centered triple ring equilibria, including the $n=2$ case, where the vortices are arranged on perpendicular lines, the unique centered triple ring for $n=6$ (this configuration is given in the Los Alamos catalog as the linearly stable 19_1), the three centered triple rings for $n=8$ [Fig. 12(c) is listed in the Los Alamos catalog as the linearly stable configuration 25_6], and the five centered triple rings for $n=9$.

We remarked above that the points of intersection of (34a) with the R_1 or R_2 axis correspond to staggered configurations of two n-gons with a vortex of strength $n\Gamma$ at the center. We noted that such states only exist for $n \geqslant 17$. Similarly, the points of intersection of (34a′) with the R_1 or R_2 axis correspond to staggered configurations of two n-gons with a vortex of strength $(n+1)\Gamma$ at the center. One might think that the addition of a single unit of circulation at the center would be insignificant so far as the existence of such an equilibrium is concerned (although the values of the radii might change). However, this addition turns out to have a substantial effect. We find that one must have $n \geqslant 20$ before a centered, staggered configuration of the type in question is possible.

C. The degenerate case for three centered, nested polygons

The degenerate case of centered triple rings requires us to solve (32′) and two of

$$(2R_1^2 - 5n - 1)(2R_2^2 - n - 1)R_1^{2n} = (2R_2^2 - 5n - 1)(2R_1^2 - n - 1)R_2^{2n}, \tag{38a'}$$

$$(2R_2^2 - 5n - 1)(2R_3^2 - n - 1)R_2^{2n} = (2R_3^2 - 5n - 1)(2R_2^2 - n - 1)R_3^{2n}, \tag{38b'}$$

$$(2R_3^2 - 5n - 1)(2R_1^2 - n - 1)R_3^{2n} = (2R_1^2 - 5n - 1)(2R_3^2 - n - 1)R_1^{2n}. \tag{38c'}$$

The angle condition is now

$$F_1 + F_2 e^{in(\phi_2 - \phi_1)} + F_3 e^{in(\phi_3 - \phi_1)} = 0, \tag{39a'}$$

where

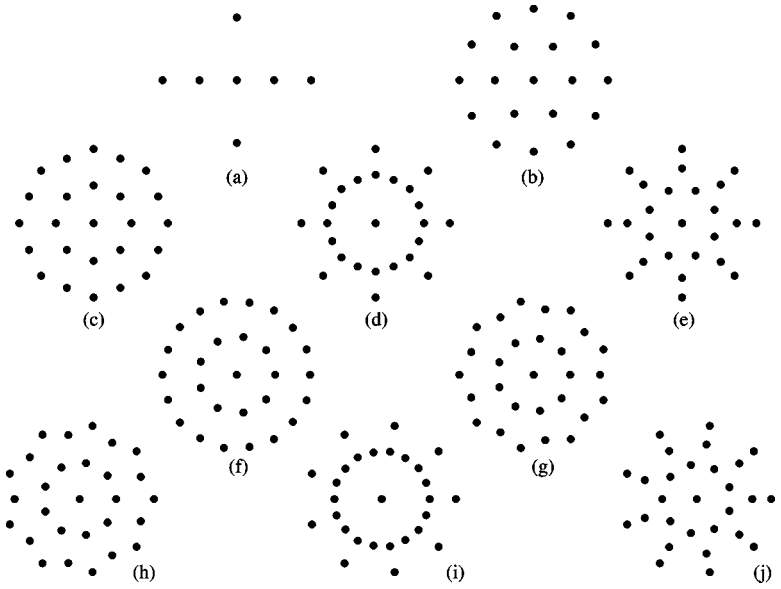

FIG. 12. Centered, nested, staggered n-gon configurations. The single configuration for (a) $n=2$, (b) $n=6$ (Los Alamos catalog 19_1). (c)–(e) The three configurations for $n=8$ [panel (c) is Los Alamos catalog 25_6]. (f)–(j) The five configurations for $n=9$.

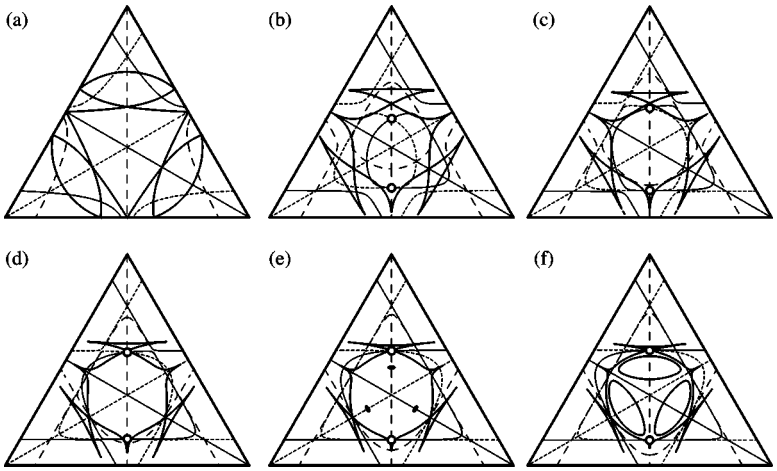

FIG. 13. Trilinear diagram plots for the "degenerate case" of three centered, nested n-gons when (a) $n=3$, (b) 4, (c) 5, (d) 6, (e) 7, and (f) 8.

$$F(R) = (2R^2 - 5n - 1)R^n = f(R) - 2R^n \tag{42}$$

[cf. (31d)]. The solutions combine aspects of "the centered case" analyzed above and the degenerate case analyzed in Sec. VI D.

Figure 13, the counterpart of Fig. 9, shows examples of the trilinear diagrams for $n=3$, 4, 5, 6, 7, and 8. Again, forbidden islands emerge. The pattern, established by the time we reach $n=6$, of having two solution points (apart from the trivial $R_1=R_2=R_3$) within the boundary defined by the angle condition (39c) appears to persist for higher n. We conclude that there are two solutions of this family for each n. Once again, these solutions all have two radii equal. Interestingly, there is no solution for $n=3$ (other than all vortices being on the same ring).

As n increases we have to ever better accuracy that the two solutions are given by an extension of (37′):

$$F': \quad R_1 \approx \sqrt{\frac{5n+1}{2}}, \quad R_2 = R_3 \approx \sqrt{\frac{2n+1}{2}},$$

$$G': \quad R_1 \approx \sqrt{\frac{n+1}{2}}, \quad R_2 = R_3 \approx \sqrt{\frac{4n+1}{2}}.$$

Figure 14 provides sample configurations for $n=4$, 5, 6, 7, 8, and 9. Some of these appear in the Los Alamos catalog. Thus, the $n=5$ configuration in Fig. 14(c) is the linearly stable 16_2 of the catalog and the $n=6$ configuration, Fig. 14(e), is the linearly unstable 19_2. (Interestingly the more symmetric, centered, staggered three-ring configuration in Fig. 12(b) is linearly stable.) The configuration in Fig. 14(g) appears in the Los Alamos catalog as the linearly unstable 22_2. [Again, the more symmetric, centered, staggered three-ring configuration, the $n=7$ counterpart of Fig. 12(b) or 12(c), is linearly stable.] Finally, Fig. 14(i) is configuration 28_7 of the Los Alamos catalog, listed as linearly unstable.

VIII. CONCLUSIONS AND DISCUSSION

Using an analytical method of moment equations, which may have broader applicability, we have achieved a rather comprehensive analytical understanding of a family of "vortex crystals" wherein identical vortices are distributed on three concentric, regular polygons with or without a vortex in the center. Even though the geometry in these states is constrained, there remains a measure of richness in the solutions, particularly in the case where one of the three rings is staggered relative to the other two. The analysis allows us to describe precisely several of the states found numerically and reported previously in the literature, particularly in the comprehensive collection known as the Los Alamos catalog.

It may be beneficial to summarize the results in a table giving for each n the number of different configurations in the different categories that we have explored, viz., symmetric, staggered, degenerate, centered symmetric, centered staggered, and centered degenerate. This summary may be found in Table III.

Perusing the catalog with the benefit of the insights obtained here one still sees many configurations, particularly

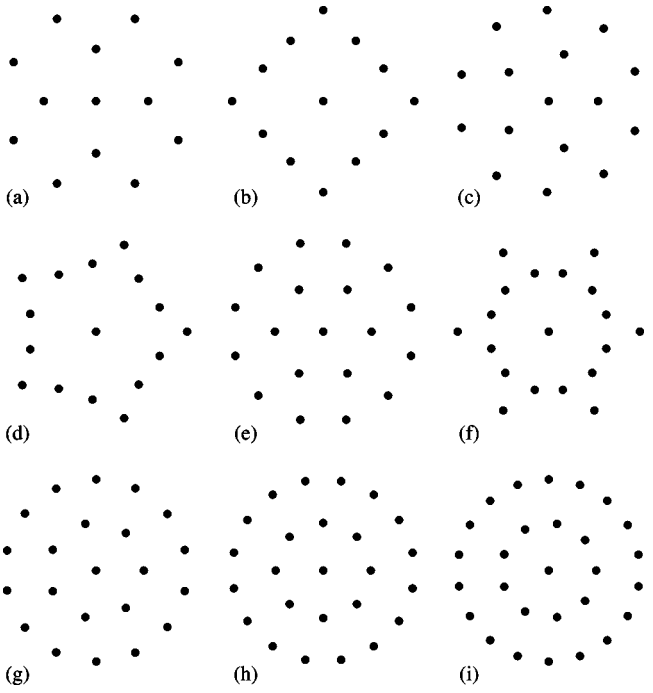

FIG. 14. Centered, nested "degenerate" triple vortex ring configurations for (a) $n=4$, (b) 4, (c) 5, (d) 5, (e) 6, (f) 7, (g) 8, and (h) 9. The second configuration for $n=7$, 8, and 9 resembles (e) but with successively more "spokes."

TABLE III. Summary of the number of states of the different kinds for increasing n. The column headings are Sym=symmetric, Stag=staggered, Deg=degenerate, C Sym=centered symmetric, C Stag=centered staggered, C Deg=centered degenerate, and the Total.

n	Sym	Stag	Deg	C Sym	C Stag	C Deg	Total
2	1	1	0	1	1	0	4
3	1	1	2	1	1	0	6
4	1	1	2	1	1	2	8
5	1	1	2	1	1	2	8
6	1	3	2	1	1	2	10
7	1	3	2	1	3	2	12
8	1	3	2	1	3	2	12
$\geqslant 9$	1	5	2	1	5	2	16

those of low symmetry, for which we have no analytical understanding whatsoever. Later additions to this list include, of course, the asymmetric configurations found by Aref and Vainchtein.[11]

We have discussed linear stability issues only in passing although historically these have been paramount in the analyses of vortex equilibria. In Ref. 1 it is argued that this emphasis is somewhat misplaced, and examples are given of how unstable equilibria often play a significant role in the dynamics of few-vortex systems. When a configuration is included in the Los Alamos catalog, we have cited the result of the linear stability calculation provided there. According to these results most of the triple rings found appear to be linearly unstable.

It is important to stress the geometrical restriction to nested, regular n-gons underlying the analysis in much of this paper. There are equilibria in which the vortices are arranged on three rings that are not captured by the above analysis because the vortices do not form regular polygons. We give four examples in Fig. 15, two each with eight and ten vortices. These states clearly have the vortices distributed on three circles and, in that sense, are "vortex triple rings."

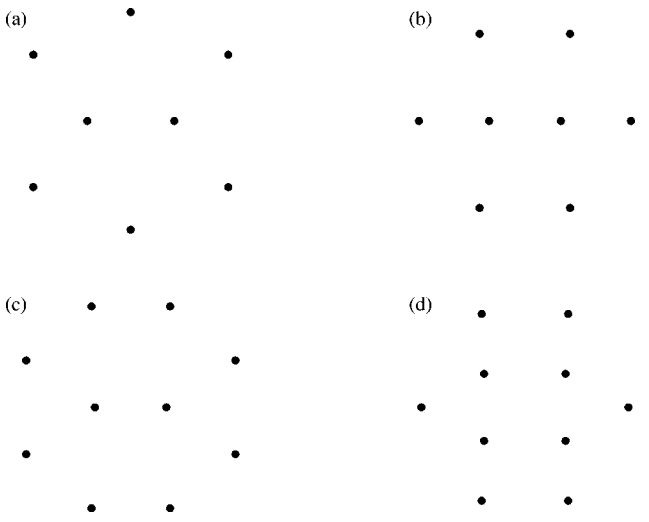

FIG. 15. Examples of equilibria in which the vortices are arranged on three concentric rings but do not form regular polygons. (a) $n=8$, (b) 8, (c) 10 (this is configuration 10_2 in the Los Alamos catalog), and (d) 10. These states include quadrilaterals that are not squares.

However, the four vortices on the same circle in these configurations are not arranged in a square. The moment method pursued herein can be applied to determine the coordinates of these configurations analytically. In Appendix we show how to obtain the two configurations for eight vortices shown in the top row of Fig. 15 and, in the process, to show that there are no others with that particular symmetry.

ACKNOWLEDGMENT

This paper is dedicated to Professor H. Keith Moffatt on the occasion of his seventieth birthday.

APPENDIX: DETERMINATION OF EIGHT-VORTEX EQUILIBRIA SHOWN IN FIG. 15

Let us apply the moment method outlined in Sec. III to configurations in which the vortices appear in pairs at diametrically opposite points, i.e., $N=2n$ and the vortex positions are $\pm z_\alpha$, $\alpha=1,\ldots,n$. We may think of this as n-nested digons. Hence, Eq. (20) with all $n_s=2$ gives

$$\sum_{\alpha=1}^{n}(2|z_\alpha|^2-1)\nu_\alpha=\sum_{\substack{\alpha,\beta=1\\ \alpha\neq\beta}}^{n}\nu_\alpha\nu_\beta, \tag{A1}$$

where the notation ν_α means

$$\nu_\alpha=\frac{2}{1-(Xz_\alpha)^2},$$

cf. (18a). We may now study Eq. (A1) for increasing values of n.

For $n=1$ we have just two vortices at $\pm z$, where $|z|=1/\sqrt{2}$. Any configuration with the two vortices at equal distances from the origin is a steadily rotating state.

For $n=2$ ($N=4$) Eq. (A1) gives specializations for $n=2$ of Eqs. (21a), (22a), and (22b), since $|z_\alpha|=R_\alpha$, a notation that we shall use henceforth. For $n=3$ we get, similarly, equations that have already been derived and discussed previously, viz., Eq. (30) with what is there called n set to 2.

We break a new ground with $n=4$. Our basic Eq. (A1) now reads

$$(2R_1^2-1)\nu_1+(2R_2^2-1)\nu_2+(2R_3^2-1)\nu_3+(2R_4^2-1)\nu_4$$
$$=2(\nu_1\nu_2+\nu_2\nu_3+\nu_3\nu_1+\nu_1\nu_4+\nu_2\nu_4+\nu_3\nu_4). \quad \text{(A2)}$$

Clearing the denominators we have

$$(2R_1^2-1)(1-X^2z_2^2)(1-X^2z_3^2)(1-X^2z_4^2)+(2R_2^2-1)(1-X^2z_1^2)(1-X^2z_3^2)(1-X^2z_4^2)+(2R_3^2-1)(1-X^2z_1^2)(1-X^2z_2^2)(1-X^2z_4^2)$$
$$+(2R_4^2-1)(1-X^2z_1^2)(1-X^2z_2^2)(1-X^2z_3^2)$$
$$=4[(1-X^2z_1^2)(1-X^2z_2^2)+(1-X^2z_2^2)(1-X^2z_3^2)+(1-X^2z_3^2)(1-X^2z_1^2)+(1-X^2z_1^2)(1-X^2z_4^2)+(1-X^2z_2^2)(1-X^2z_4^2)$$
$$+(1-X^2z_3^2)(1-X^2z_4^2)]. \quad \text{(A3)}$$

The right-hand side may be simplified to

$$4[6-3X^2(z_1^2+z_2^2+z_3^2+z_4^2)+X^4(z_1^2z_2^2+z_2^2z_3^2+z_3^2z_1^2+z_1^2z_4^2$$
$$+z_2^2z_4^2+z_3^2z_4^2)]. \quad \text{(A4)}$$

Setting the overall coefficient of each power of X to zero in (A3) we obtain

$$R_1^2+R_2^2+R_3^2+R_4^2=14, \quad \text{(A5a)}$$

$$(15-2R_2^2-2R_3^2-2R_4^2)z_1^2+(15-2R_1^2-2R_3^2-2R_4^2)z_2^2$$
$$+(15-2R_1^2-2R_2^2-2R_4^2)z_3^2$$
$$+(15-2R_1^2-2R_2^2-2R_4^2)z_4^2=0, \quad \text{(A5b)}$$

$$(R_3^2+R_4^2-3)z_1^2z_2^2+(R_1^2+R_4^2-3)z_2^2z_3^2+(R_2^2+R_4^2-3)z_3^2z_1^2$$
$$+(R_2^2+R_3^2-3)z_1^2z_4^2+(R_1^2+R_3^2-3)z_2^2z_4^2$$
$$+(R_1^2+R_2^2-3)z_3^2z_4^2=0, \quad \text{(A5c)}$$

$$(2R_1^2-1)z_2^2z_3^2z_4^2+(2R_2^2-1)z_1^2z_3^2z_4^2+(2R_3^2-1)z_1^2z_2^2z_4^2$$
$$+(2R_4^2-1)z_1^2z_2^2z_3^2=0. \quad \text{(A5d)}$$

Using the first of these in the second and the third we obtain

$$(2R_1^2-13)z_1^2+(2R_2^2-13)z_2^2+(2R_3^2-13)z_3^2$$
$$+(2R_4^2-13)z_4^2=0, \quad \text{(A5b′)}$$

$$(R_1^2+R_2^2-11)z_1^2z_2^2+(R_2^2+R_3^2-11)z_2^2z_3^2$$
$$+(R_3^2+R_1^2-11)z_3^2z_1^2+(R_1^2+R_4^2-11)z_1^2z_4^2$$
$$+(R_2^2+R_4^2-11)z_2^2z_4^2+(R_3^2+R_4^2-11)z_3^2z_4^2=0, \quad \text{(A5c′)}$$

$$\frac{2R_1^2-1}{z_1^2}+\frac{2R_2^2-1}{z_2^2}+\frac{2R_3^2-1}{z_3^2}+\frac{2R_4^2-1}{z_4^2}=0. \quad \text{(A5d′)}$$

Let us now specialize to the cases illustrated in Fig. 15 where for eight vortices we have configurations—until now only known from numerical experiments—in which in our current notation z_1 is real, z_2 is either real or pure imaginary, and z_3 and z_4 are complex conjugates. We have, therefore, two cases to explore (i) $z_1=x_1$, $z_2=x_2$, $z_3=\xi+i\eta$, and $z_4=\xi-i\eta$; and (ii) $z_1=x$, $z_2=iy$, $z_3=\xi+i\eta$, and $z_4=\xi-i\eta$.

In case (i) the equations above reduce to

$$x_1^2+x_2^2+2R^2=14, \quad \text{(A6a)}$$

$$(2x_1^2-13)x_1^2+(2x_2^2-13)x_2^2+(2R^2-13)(\zeta^2+\overline{\zeta^2})=0, \quad \text{(A6b)}$$

$$(x_1^2+x_2^2-11)x_1^2x_2^2+(x_2^2+R^2-11)x_2^2\zeta^2$$
$$+(x_1^2+R^2-11)x_1^2\zeta^2+(x_1^2+R^2-11)x_1^2\overline{\zeta^2}$$
$$+(x_2^2+R^2-11)x_2^2\overline{\zeta^2}+(2R^2-11)R^4=0, \quad \text{(A6c)}$$

$$4-\frac{1}{x_1^2}-\frac{1}{x_2^2}+\frac{2R^2-1}{R^4}(\zeta^2+\overline{\zeta^2})=0, \quad \text{(A6d)}$$

where $\zeta=\xi+i\eta$, and $R=|\zeta|$. The third of these can be simplified further,

$$(x_1^2+x_2^2-11)x_1^2x_2^2+[x_1^4+x_2^4+(R^2-11)(x_1^2+x_2^2)](\zeta^2+\overline{\zeta^2})$$
$$+(2R^2-11)R^4=0.$$

We may use

$$x_1^4+x_2^4=(x_1^2+x_2^2)^2-2x_1^2x_2^2=4(7-R^2)^2-2x_1^2x_2^2$$

and (A6a) to eliminate the sum of the fourth powers and the sum of the squares of x_1 and x_2 in favor of R. In this way we produce the following three equations:

$$8(7-R^2)^2-4x_1^2x_2^2-26(7-R^2)+(2R^2-13)(\zeta^2+\overline{\zeta^2})=0, \quad \text{(A7a)}$$

$$(3-2R^2)x_1^2x_2^2+2(R^4-10R^2+21-x_1^2x_2^2)(\zeta^2+\overline{\zeta^2})$$
$$+(2R^2-11)R^4=0, \quad \text{(A7b)}$$

$$4x_1^2x_2^2R^4-2(7-R^2)R^4+(2R^2-1)x_1^2x_2^2(\zeta^2+\overline{\zeta^2})=0, \quad \text{(A7c)}$$

involving the three quantities $(x_1x_2)^2$, R^2, and $\zeta^2+\overline{\zeta^2}$. The unique solution of Eqs. (A7) for which $(\zeta^2+\overline{\zeta^2})/2R^2$ is numerically less than 1 is found to be

$$x_1x_2=1.672\,596\,148\,5, \quad R=2.059\,269\,991\,7,$$

$$\zeta^2 + \overline{\zeta^2} = -4.873\,020\,829\,3,$$

to ten decimal places. From this we easily get the vortex coordinates

$$\pm 1.827\,170\,396\,2, \quad \pm 0.949\,758\,517\,8,$$

$$0.0, \quad \pm 2.225\,784\,485\,3,$$

$$0.0, \quad \pm 0.751\,463\,656\,7, \tag{A8}$$

which agree with the values previously found by direct numerical solution of Eq. (1) using the "ghost vortex method" of Aref and Vainchtein.[11] This configuration is shown in Fig. 15(b).

Case (ii) proceeds similarly. The counterparts of Eqs. (A6) are

$$x^2 + y^2 + 2R^2 = 14, \tag{A9a}$$

$$(2x^2 - 13)x^2 - (2y^2 - 13)y^2 + (2R^2 - 13)(\zeta^2 + \overline{\zeta^2}) = 0, \tag{A9b}$$

$$\begin{aligned} &-(x^2 + y^2 - 11)x^2y^2 - (y^2 + R^2 - 11)y^2\zeta^2 \\ &\quad + (x^2 + R^2 - 11)x^2\zeta^2 + (x^2 + R^2 - 11)x^2\overline{\zeta^2} \\ &\quad - (y^2 + R^2 - 11)y^2\overline{\zeta^2} + (2R^2 - 11)R^4 = 0, \end{aligned} \tag{A9c}$$

$$-\frac{1}{x^2} + \frac{1}{y^2} + \frac{2R^2 - 1}{R^4}(\zeta^2 + \overline{\zeta^2}) = 0. \tag{A9d}$$

We use the transformation

$$x^4 - y^4 = (x^2 + y^2)(x^2 - y^2) = 2(7 - R^2)(x^2 - y^2)$$

to produce from (A9) the following counterparts of Eqs. (A7):

$$(15 - 4R^2)(x^2 - y^2) + (2R^2 - 13)(\zeta^2 + \overline{\zeta^2}) = 0, \tag{A10a}$$

$$(2R^2 - 3)x^2y^2 + (3 - R^2)(x^2 - y^2)(\zeta^2 + \overline{\zeta^2}) + (2R^2 - 11)R^4 = 0, \tag{A10b}$$

$$(x^2 - y^2)R^4 + x^2y^2(2R^2 - 1)(\zeta^2 + \overline{\zeta^2}) = 0. \tag{A10c}$$

From (A10a) and (A10c) we get either (a) $x^2 = y^2$, i.e., $x = y = a$, since we can choose the signs of x and y by relabeling the vortices, or (b)

$$x^2y^2 = -\frac{2R^2 - 13}{(2R^2 - 1)(4R^2 - 15)}R^4, \tag{A11a}$$

$$x^2 - y^2 = \pm 2R^2\sqrt{\frac{(2R^2 - 13)(4R^6 - 40R^4 + 109R^2 - 51)}{(R^2 - 3)(2R^2 - 1)(4R^2 - 15)^2}}. \tag{A11b}$$

In order to obtain (A11a), we combined (A10a) and (A10c), while (A11b) is derived from (A10b) using (A11a) and (A10a). We now note that

$$4x^2y^2 = (x^2 + y^2)^2 - (x^2 - y^2)^2 = 4(7 - R^2)^2 - (x^2 - y^2)^2. \tag{A11c}$$

In case (a) this [or (A9a)] implies that the common value of x and y, called a above, is given by

$$a^2 = 7 - R^2.$$

Substituting this value into (A10b) gives an equation for R, viz.,

$$(2R^2 - 3)(7 - R^2)^2 + (2R^2 - 11)R^4 = 0,$$

or

$$4R^6 - 42R^4 + 140R^2 - 147 = 0,$$

a cubic equation in R^2 that has three real, positive roots, $R^2 = 7/2$, and $(7 \pm \sqrt{7})/2$. The polar angle ϕ of vortex 3, given in general by

$$\frac{\zeta^2 + \overline{\zeta^2}}{2R^2} = \cos 2\phi,$$

is $\pi/4$ since the left-hand side vanishes. Thus, vortices 1 and 2 and their opposites are on the x and y axes, respectively, vortices 3 and 4 and their opposites are on the lines $x = \pm y$. If $R^2 = 7/2$, $a = R$ and the vortices form the regular octagon. If $R^2 = (7 + \sqrt{7})/2$, $a^2 = (7 - \sqrt{7})/2$, and the configuration consists of two nested squares. The last possibility $R^2 = (7 - \sqrt{7})/2$, $a^2 = (7 + \sqrt{7})/2$, again leads to two nested squares with the vortices relabeled.

In case (b) substitution of (A11a) and (A11b) into (A11c) yields an equation for R^2. After some elementary transformations this equation becomes

$$\begin{aligned} &4(2R^2 - 13)(R^2 - 1)(R^2 - 4)(R^2 - 6)R^4 \\ &\quad = (R^2 - 3)(2R^2 - 1)(4R^2 - 15)^2(R^2 - 7)^2, \end{aligned} \tag{A12}$$

or

$$\begin{aligned} &8R^{12} - 220R^{10} + 2330R^8 - 11\,985R^6 + 30\,693R^4 \\ &\quad - 34\,755R^2 + 11\,025 = 0. \end{aligned}$$

This equation has six real, positive solutions. For each of them we can check the value of

$$\frac{\zeta^2 + \overline{\zeta^2}}{2R^2} = \cos 2\phi,$$

where ϕ is the polar angle of vortex 3. If the ratio on the left-hand side is between -1 and $+1$, we have a possible equilibrium configuration. It turns out that only for one solution of (A12), $R^2 = 4.685\,491\,369\,0$, is this the case. We now easily produce the coordinates of this configuration

$$\pm 1.215\,717\,238\,5, \quad \pm 1.790\,955\,880\,2,$$

$$\pm 1.997\,963\,458\,2, \quad 0.0,$$

$$0.0, \quad \pm 0.798\,222\,576\,5. \tag{A13}$$

This configuration was shown in Fig. 15(a).

One could argue that because of the extreme symmetry of these configurations their analytical determination could

be obtained directly from the basic Eq. (1). However, if this is attempted, the intervortex distances are complicated to handle. The moment method allows a more transparent approach to finding the values of the coordinates.

[1]H. Aref, P. K. Newton, M. A. Stremler, T. Tokieda, and D. L. Vainchtein, "Vortex crystals," Adv. Appl. Mech. **39**, 1 (2002).
[2]P. K. Newton, *The N-Vortex Problem—Analytical Techniques*, Applied Mathematical Sciences Vol. 145 (Springer, Berlin, 2001).
[3]P. G. Saffman, *Vortex Dynamics* (Cambridge University Press, Cambridge, 1992), p. 311.
[4]J. P. Kossin and W. H. Schubert, "Mesovortices in hurricane Isabel," Bull. Am. Meteorol. Soc. **85**, 151 (2004).
[5]T. H. Havelock, "The stability of motion of rectilinear vortices in ring formation," Philos. Mag. **11**, 617 (1931).
[6]L. J. Campbell and R. M. Ziff, Los Alamos Scientific Laboratory informal report LA-7384-MS, Rev. (1979), p. 40.
[7]E. J. Yarmchuk, M. J. V. Gordon, and R. Packard, "Observation of stationary vortex arrays in rotating superfluid helium," Phys. Rev. Lett. **43**, 214 (1979).
[8]L. J. Campbell and R. M. Ziff, "Vortex patterns and energies in a rotating superfluid," Phys. Rev. B **20**, 1886 (1979).
[9]F. Cajori, *An Introduction to the Theory of Equations* (Dover, New York, 1969), p. 239.
[10]H. Aref, "Trilinear coordinates in fluid mechanics," in *Studies in Turbulence*, edited by T. B. Gatski, S. Sarker, and C. G. Speziale (Springer, Berlin, 1992), pp. 568–581.
[11]H. Aref and D. L. Vainchtein, "Point vortices exhibit asymmetric equilibria," Nature (London) **392**, 769 (1998).